COMPARATIVE STUDY BETWEEN AZIMUTH-ELEVATION AND TILT-ROLL SUN-TRACKING SYSTEMS IN RANGE OF MOTION

WANG TZE KOON

UNIVERSITI TUNKU ABDUL RAHMAN

COMPARATIVE STUDY BETWEEN AZIMUTH-ELEVATION AND TILT-ROLL SUN-TRACKING SYSTEMS IN RANGE OF MOTION

WANG TZE KOON

A project report submitted in partial fulfilment of the requirements for the award of Bachelor of Engineering (Hons.) Electrical and Electronic Engineering

Lee Kong Chian Faculty of Engineering and Science
Universiti Tunku Abdul Rahman

August 2017

DECLARATION

I hereby declare that this project report is based on my original work except for citations and quotations which have been duly acknowledged. I also declare that it has not been previously and concurrently submitted for any other degree or award at UTAR or other institutions.

Signature	:	
Name	:	Wang Tze Koon
ID No.	:	12UEB02661
Date	:	18th September 2017

APPROVAL FOR SUBMISSION

I certify that this project report entitled **"COMPARATIVE STUDY BETWEEN AZIMUTH-ELEVATION AND TILT-ROLL SUN-TRACKING SYSTEMS IN RANGE OF MOTION"** was prepared by **WANG TZE KOON** has met the required standard for submission in partial fulfilment of the requirements for the award of Bachelor of Engineering (Hons.) Electrical and Electronic Engineering at Universiti Tunku Abdul Rahman.

Approved by,

Signature	:	
Supervisor	:	Dr. Wong Chee Woon
Date	:	18th September 2017

ACKNOWLEDGEMENTS

I would like to express my deepest appreciation to my supervisor, Dr Wong Chee Woon whose contribution in stimulating suggestions and encouragement, helped me to coordinate my project especially in writing this report and present my content in poster. Also I would like to express my gratitude to the committee and staff of poster competition, who gave me the opportunity to present my project in the public.

ABSTRACT

In the solar concentrator industry, dual-axis sun-tracking system is essential to maximize the production of solar energy. However, there are inevitable parasitic energy losses from the sun-tracking motors. In this study, the parasitic energy losses of all kinds of dual-axis sun-tracking systems, e.g. azimuth-elevation dual-axis sun-tracking system (AE-DAST), polar dual-axis sun-tracking system (P-DAST) and horizontal (H-DAST) dual-axis sun-tracking system, have been investigated in term of the range of motion of the sun-tracking system. Algorithms were developed to evaluate and compare the annual accumulated range of motion (AROM) of the sun-tracking systems with respect to various locations for latitudes ranging from 45°N to 45°S. Two manipulated parameters, which are the stow position and offset hours were introduced to compare and analyse the range of motion of the three dual-axis sun-tracking systems. Stow position defined as the parking position for photovoltaic (PV) panel before and after sun-tracking process. It is categorised as fixed and non-fixed stow positions. With fixed stow position, the PV panel has to stow at a position parallel to ground whereas for the case of non-fixed stow position, the PV panel halted before sunset and start the sun-tracking process again from this position. This approach is introduced to compare and justify the best stow position in the range of motion (ROM) for various location in order to mitigate the possibility of wind load after a sun-tracking period. Offset hours is considered to control the tracking starting and ending time of the sun-tracking process in order to investigate and identify the suitable offset hours for various location. Net energy defined as the difference between energy generated by PV and motor energy consumption are introduced in order to accurately identify the suitable tracking system associated with the chosen parameters for various location. As a result, AROM varies with latitudes. Fixed stow position experience more parasitic energy losses as compare to non-fixed stow position. P-DAST and H-DAST are the best options for latitudes ranging from 15°S to 15°N and latitudes above 15°N and below 15°S respectively for fixed stow position. In the case of non-fixed stow position, P-DAST experience the least parasitic energy losses and thus it is the best option as compared to AE-DAST and H-DAST. With referenced to zero offset hours, the difference in energy generated for one, two and three hours are within the range of 1% to 3.13%, 5.14% to 12.25% and 17.32% to 26.99% respectively. This approach allows the solar

concentrator system designer to optimize the system efficiency by determining the sun-tracking system with the least parasitic energy losses.

TABLE OF CONTENTS

LIST OF TABLES

LIST OF FIGURES

LIST OF SYMBOLS / ABBREVIATIONS

η_{con}	electrical conversion efficiency
n_{rpm}	motor rotational speed
η_{op}	optical efficiency
$\mathrm{P}_{\mathrm{m,p}}$	primary motor power consumption
$\mathrm{P}_{\mathrm{m,s}}$	secondary motor power consumption
t_s	solar time
π	180 degree
δ	declination angle
ω	hour angle
Φ	latitude angle
β	primary (azimuth) angle
α	secondary (elevation) angle
A	solar concentrator reflective area
AE-DAST	azimuth-elevation dual-axis sun-tracking system
AROM	accumulated range of motion
D	daylight saving
DNI	direct normal irradiance
EOT	equation of time, minutes
GR	gear ratio
H-DAST	horizontal dual-axis sun-tracking system
HSAT	horizontal single axis tracker
LCT	local clock time
LC	longitude correction, °
PASAT	polar aligned single-axis tracker
P-DAST	polar dual-axis sun-tracking system
ROM	range of motion
TSAT	tilted single axis tracker
VSAT	vertical single axis tracker

LIST OF APPENDICES

CHAPTER 1

INTRODUCTION

1.1 General Introduction

With the advancement of technology, renewable energy can be easily obtained and process into useful energy such as electricity, heat, oil and gas etc. The energy demand has increased year by year and at the same time, the existing sources of petroleum and fossil fuels continue to decrease. According to the energy information administration (IER, 2016), the mostly used renewable energies are hydropower (25%), biomass (48%), wind (19%), geothermal (2%) and solar (5%) where, hydropower, wind and solar develop in fast paces, especially solar energy, the most abundant form of renewable energy. Although solar energy became commonly used in the present era, it is however subject to a few factors. In order to obtain maximum solar energy from the PV system, the location (latitude) is an important factor to be considered.

Figure 1.1 below shows the world wide data set of direct normal irradiance from NASA Surface Meteorology and Solar Energy Program (SSE) (Trieb *et al.*, 2009). It illustrate the locations that has the potential to implement concentrating PV system where direct normal irradiation define as the solar radiation received by the solar panel is perpendicular to the rays from the sun in a straight line direction.

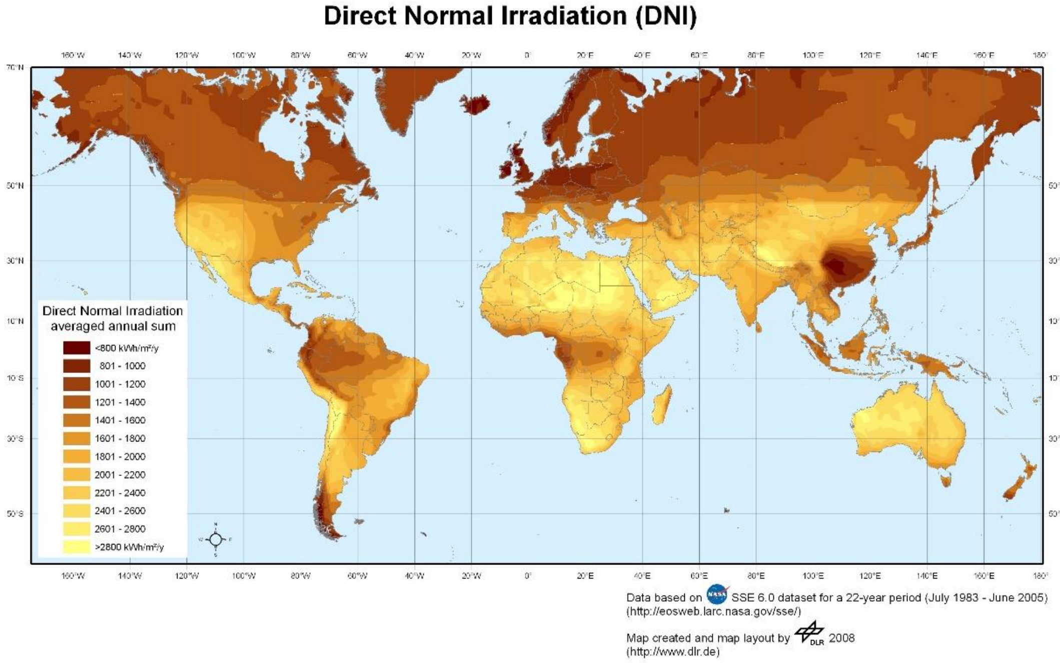

Figure 1.1: Worldwide annual direct normal irradiation in kWh/m2/year from NASA SSE (Trieb *et al.*, 2009)

From Figure 1.1 above, it is noticed that countries located above latitude 50˚N and countries located below 50˚S has the least direct normal irradiation obtained throughout the year with an average annual direct normal irradiation of at most 1200 kWh/m^2/year. For countries located ranging from 30˚S to 50˚N has greater potential to implement concentrating PV system with an average annual direct normal irradiation ranging from 1801 to 2800 kWh/m^2/year.

1.2 Importance of the Study

Until now, many countries around the world still using fossil fuels which are expected to be exhausted by the end of 21st Century (Terra Symbiosis, 2000). Therefore, renewable energy such as hydropower, wind and solar energy has to pick up to cover the energy demand for the next century.

Other countries located at north hemisphere and south hemisphere obtain the least sun energy because the earth can only tilted on certain declination angle. Therefore sun-tracking system are invent to ensure maximum sun energy collected by the PV system at countries that are least cover by the sun radiation.

Sun-tracking system categorised into two which are the single and dual-axis sun tracker. There are a few types of single-axis sun tracker normally used which are the vertical, tilted, polar aligned and horizontal single-axis tracker. Single-axis sun tracker track the sun movement along east-west direction only. Sun will not move in a straight line along the sun path, thus it is possible to have cosine loss as the sun rays is not perpendicular towards the solar panel and consequently amount of sun irradiance collected is less. Therefore, dual-axis sun-tracking system invent to overcome this problem. Dual-axis sun tracker consists of two tilted angle which allows the tracker to have two degrees of freedom tracking from east to west. Dual-axis sun tracker inherent the ability to tilt the panel in four trigonometric quadrants. Dual-axis sun tracker such as azimuth-elevation (AE) are commonly used sun-tracking system. In this project, varies types of sun-tracking system are studied to understand the behaviour of each type of sun tracking systems in range of motion such as azimuth-elevation dual-axis sun-tracking system (AE-DAST) and polar dual-axis sun-tracking system (P-DAST). Moreover, horizontal dual-axis sun-tracking system (H-DAST) is consider to compare with other two dual-axis sun-tracking system in range of motion accumulated. This is to provide another option for solar concentrator industry.

1.3 Problem Statement

In order to maximize the production of solar energy, dual-axis sun-tracking system is introduced to overcome the unavailability of single-axis sun tracker in which the latter only able to track sun movement in one direction from east to west. However, there are inevitable parasitic losses due to dual-axis sun tracker as it require two motor to drive the tracking system. Parasitic losses refer to the power loss in system that is unavoidable.

As single-axis sun-tracking system required only one motor to operate, therefore less parasitic losses as compare to dual-axis tracker. However, it cannot maximize the production of solar energy as compare to single-axis sun tracker. Therefore, it is important to seek a balance between the production of solar energy and motor power consumption. Hence, range of motion for all kinds of dual-axis sun-tracking system are studied. Algorithm has been developed to study the accumulated range of motion with respect to various latitudes from 45°N to 45°S. Besides that, a few conditions were introduced to study the behaviour of all kinds of tracking system such as stow position and starting and ending time. The general knowledge on advantages and disadvantages of single and dual-axis are as follows.

Advantages and Disadvantage of single-axis and dual-axis sun tracker

Table 1.1: Advantages and Disadvantage of single-axis and dual-axis sun tracker

Type of Tracker	Advantages	Disadvantages
Single-axis Sun Tracker	- Required less motor power consumption - Low cost and simple design	- Only able to track sun movement in one direction - Low absorption of sun energy
Dual-axis Sun Tracker	- Two degree of freedom tracking system - Able to maximum production of solar energy	- More motor power consumption - Sophisticated design and construction

1.4 Aims and Objectives

The aim of this project is to study, analyse and justify the suitable type of dual-axis sun-tracking system by analysed the annual accumulated range of motions with respect to various location from 45°N to 45°S. The analysis conducted by using the powerful engineering tool, MATLAB. The objectives of the project are as follows:

(i) To study the general sun-tracking formula for various kind of on-axis sun tracker.

(ii) To design and develop an algorithm to calculate the annual accumulated range of motion of all kinds of dual axis sun tracking systems with integration of general sun-tracking formula.

(iii) To investigate and compare the performances of all kinds of dual-axis sun-tracking systems with respect to different locations.

CHAPTER 2

LITERATURE REVIEW

2.1 Sun-Tracking Tracker

Sun tracker is a device for orienting the photovoltaic solar panel to follow the sun's movement throughout the day (Harb, 2012). There are two groups of sun trackers which are the single-axis and dual-axis trackers. The sun moves from east to west in a parabolic arc from sunrise to sunset. The sun's path in the sky varies with the season and time of the day (Harb, 2012). In short, the sun tracker has the ability to effectively track the sun's movement with the changes of season to collects maximum light intensity for electricity generation.

2.2 Important Angles Contribute to Sun Tracking Algorithm

In order to compute the sun position at different time, some essential input parameters are required such as latitude (Φ), hour angle (ω) and declination angle (δ). Other parameters to be consider in sun tracking algorithm are longitude, equation of time (EOT), longitude correction (LC), daylight saving (D) and standard time zone meridian of particular location.

2.2.1 Earth Surface Coordinate System

Earth surface coordinate system also is known as observer sun angles which consists of solar azimuth angle, solar elevation or altitude angle and solar zenith angle that contribute to the central rays along a direction towards the sun. Figure 2.1 below illustrates the three observer sun angle view from the point Q.

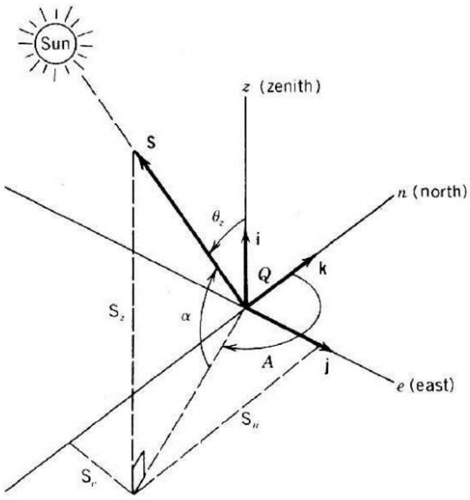

Figure 2.1: Earth Surface Coordinate System view from point Q (William and Michael, 2001)

2.2.1.1 Azimuth angle

Azimuth angle (A) is defined as the angle measured on a horizontal plane from north to the desired position at sunrise. In this case, the angle from the north represent a 0° and towards the east at 90°, south (180°), west (270°) and eventually back to the north. It can be known as primary axis rotation for sun tracking system. Primary axis rotation represents the first action taken by the sun tracking system to tilt the solar panel.

2.2.1.2 Elevation Angle

Elevation (α) also known as altitude (α) angle and it is defined as the angle between the sun ray from the central of the earth and the horizontal plane (William and Michael, 2001). It represents the angular height of the sun (Otieno, 2015). The secondary angle is zero degrees at sunrise (east), 180° at sunset (west) and 90° at solar noon. Elevation angle varies with different days and latitude angles at a particular location. Another angle named, zenith angle represent the angle between the sun ray and the polar axis. The equation can be written as follow.

$$\theta_Z = 90 - \alpha \tag{2.1}$$

The elevation angle is known as secondary angle because it represents the secondary motion of the sun tracking system after the primary axis had rotated and stopped. It tracks the sun movement by tilting the panel from east direction to west.

The secondary axis normally situated on top of the primary axis and so it is known as the secondary axis.

2.2.2 Earth Centre Coordinate System

Earth centre frame or earth centre coordinate system represents the angles measured from the centre of the earth. This system created by three essential component such as latitude angle, declination angle and hour angle. Figure 2.2 shows the coordinate system with three essential angles. Moreover, Figure 2.3 illustrates the combination of earth centre coordinate system and earth surface coordinate system.

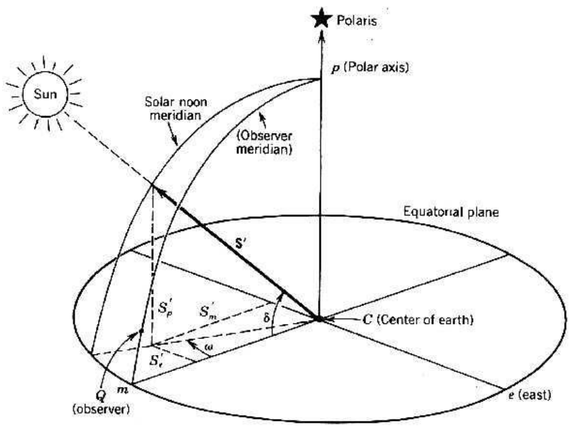

Figure 2.2: Earth Centre Coordinate System (William and Michael, 2001)

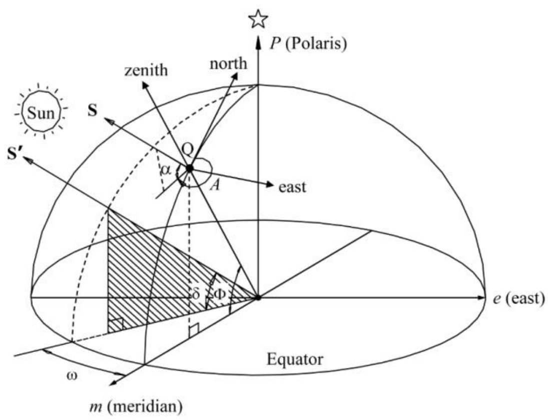

Figure 2.3: Composite view of earth centre and earth surface coordinate system (William and Michael, 2001)

2.2.2.1 Latitude Angle

Latitude (Φ) angle defined as an angle between the equatorial plane and a point on the surface of earth. Latitude angle is often used to define a country location for people to understand the exact location on earth. At the equator, the latitude angle designated as zero degrees. Latitude angle of countries located at 23.45°N and 23.45°S is known as Tropic of Cancer and Tropic of Capricorn respectively. Besides that, countries located at latitude angles of 66.55°N and 66.55°S represent the Arctic Circle and Antarctic Circle respectively (William and Michael, 2001). Countries located above Arctic Circle and below Antarctic Circle received the least sun irradiation (Trieb *et al.*, 2009).

2.2.2.2 Sun Declination Angle

Sun declination angle represents the angle between the line drawn from the centre of earth towards the sun and the equatorial planes. Figure 2.4 shows the declination angles at each seasons when the earth revolves in an elliptical orbit pattern around the sun every 365.25 days (William and Michael, 2001). The declination angle can be calculated as follow.

$$\delta = arcsin\left\{0.39795\cos\left[\frac{360}{365}(N-173)\right]\right\} \tag{2.2}$$

where N represents the number of days (i.e. $N = 1$ for 1st of January).

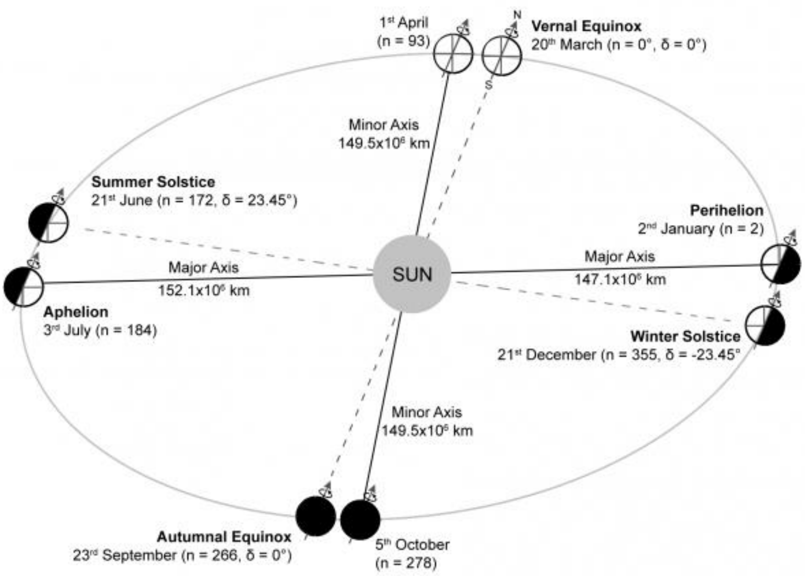

Figure 2.4: Sun declination angles at different seasons (William and Michael, 2001)

2.2.2.3 Hour Angle

Hour angle is used to describe the earth rotation about its polar axis. It is defined as the angular distance between the meridian and meridian perpendicular to the sun (William and Michael, 2001). Other relevant equations such as function of the day number (x), equation of time (EOT), longitude correction (LC) and solar time (t_s) contribute to hour angle. These equations are as follows.

The function of the day number (x):

$$x = \frac{360(N-1)}{365.242} \tag{2.3}$$

The equation of time in minutes (EOT):

$$EOT = 0.258 \times \cos x - 7.416 \times \sin x - 3.648 \times \cos 2x - 9.228 \times \sin 2x \tag{2.4}$$

The longitude correction (LC):

$$LC = \frac{(Standard\ time\ zone\ meridian) - (Local\ longitude)}{15} \tag{2.5}$$

The solar time (t_s) in 24 hours format:

$$t_s = LCT + \frac{EOT}{60} - LC - D \tag{2.6}$$

The hour angle (ω):

$$\omega = 15(t_s - 12) \tag{2.7}$$

where D represents the daylight saving in which D = 0 refer to a location that does not have daylight saving and D = 1 refer to a location that will experience daylight saving.

2.3 Type of Sun Tracking System

Sun-tracking system are categorized into two groups which are single-axis and dual-axis sun tracking systems.

2.3.1 Single-Axis Sun-Tracking System

Single-axis tracker also is known as one-axis tracker which tracks the sun's movement along one direction only. The rotational axis of sun-tracking system usually is designed to align along the meridian of the true north. It can also be designed in such a way align them with respect to any cardinal direction. The most common types of single-axis sun-tracking systems are Horizontal Single-Axis Tracker (HSAT), Vertical Single-Axis Tracker (VSAT) and Tilted Single-Axis Tracker (TSAT) as well as Polar Aligned Single-Axis Tracker (PASAT). Among all the types of single-axis trackers, HSAT and TSAT are the most common types of trackers being used (Otieno, 2015).

2.3.1.1 Horizontal Single-Axis Tracker (HSAT)

Horizontal single-axis tracker by its name, implied that the solar panel is mounted on a long cylindrical tube with bearing attached at both ends of the tube. The tube will rotate along one-axis direction to track the sun's movement from east to west. This type of tracking system usually used in the tropical region near the equator and have a high productivity during summer and spring season where the sun located at a higher altitude during noon. HSAT is not so effective at the higher latitude (above Tropic of Cancer) or lower latitude (Tropic of Capricorn) regions. The advantage of having this tracking system are the robust mechanical structure, simple design and maintenance can be done easily (Harb, 2012). Figure 2.5 below shows the horizontal single-axis sun tracker.

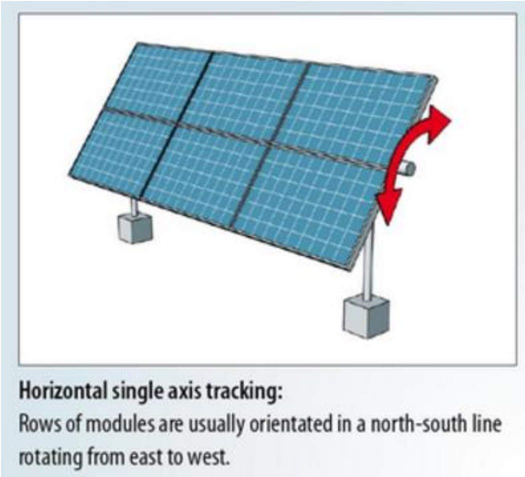

Figure 2.5: Horizontal Single-Axis Sun-Tracking Illustration (Nithya, 2015)

2.3.1.2 Vertical Single-Axis Tracker (VSAT)

For the vertical single-axis sun-tracking system, the point of rotation aligned along the polar axis. This type of tracking system also known as azimuth sun tracker in which the panel are installed at a certain degree of tilted angle between the ground. This type of sun tracker is normally used in higher latitudes (above Tropic of Cancer) regions such as the United Kingdom where the sun does not rises very high as compared to countries located near the equator, but long summer days in order for the sun to stay longer along the arc (Harb, 2012). Figure 2.6 below shows the operating mechanism of vertical (azimuth) single-axis sun-tracking system.

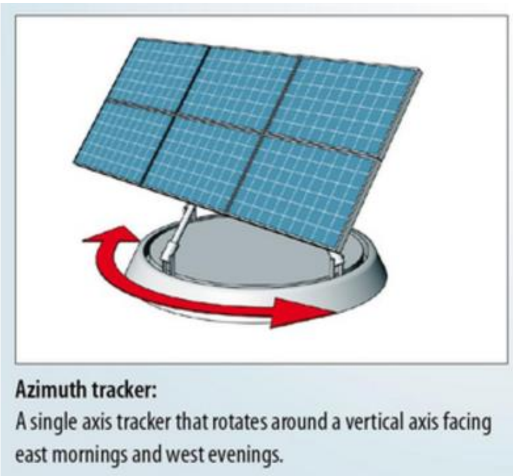

Figure 2.6: Vertical (Azimuth) Single-Axis Sun-Tracking System Illustration (Nithya, 2015)

2.3.1.3 Tilted Single-Axis Tracker (TSAT)

Vertical and horizontal axis trackers are considered as tilted single-axis tracker. This type of tracker is frequently limited in order to reduce wind disturbance. Shading issues are considered to reduce unnecessary losses and to optimize land utilisation. With tilted single-axis tracker, shading issues can be prevented by rotating the solar panel away, just enough to get rid of the shadow. This technique named back tracking in which they are packed together but without worry about shading issue (Mousazadeh *et al.*, 2009). The solar panel mounted in such a way that it is parallel to the rotation axis. However, they are limited by the site location. Tilted single-axis sun tracker illustrated in Figure 2.7 below.

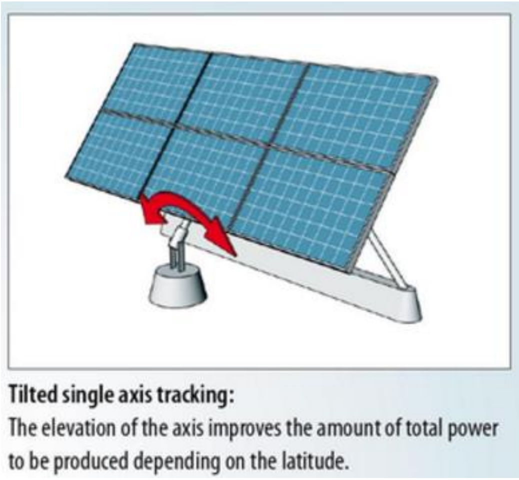

Figure 2.7: Tilted Single-Axis Sun-Tracking System Illustration (Nithya, 2015)

2.3.1.4 Polar Aligned Single-Axis Tracker (PASAT)

This type of tracking system has the ability to allow one tracking axis to aligned with respective latitude angle depend on site location. When tracking system is energized, the rotational axis automatically aligns with the earth's rotational axis. However, the principle disadvantage of this kind of tracker is because of their high wind disturbance. High mechanical stress supporting structure is required for the polar aligned single-axis tracking system.

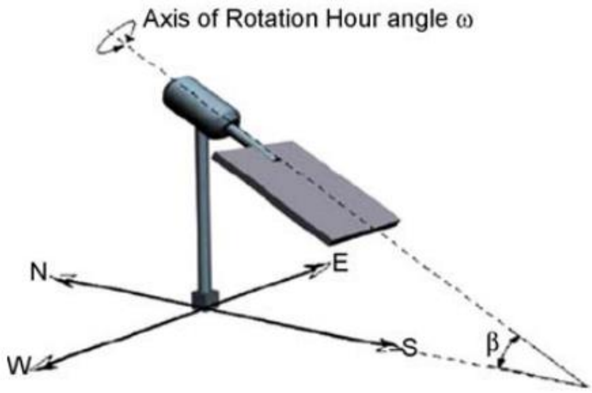

Figure 2.8: Polar Aligned Single-Axis Sun-Tracking System Illustration (Mousazadeh *et al.*, 2009)

2.3.2 Dual-Axis Sun-Tracking System

The dual-axis sun-tracking system allows the solar panel to track the sun freely in any four trigonometric quadrants, thus maximize the production of solar energy. The primary axis (azimuth) represents first rotating axis that positioned parallel with the ground. The secondary axis (elevation) refer to the second rotating axis referenced to the primary axis as it moves (Otieno, 2015). There is two types of dual-axis sun-tracking systems which are azimuth-elevation and tilt-roll dual-axis sun-tracking systems.

2.3.2.1 General Formulas for Sun Tracking System

The general formula for on-axis concentrator contributed mainly by three orientation angles or offset parameters. This formula is easy and effective to be used to study different types of dual-axis sun-tracking systems such as azimuth-elevation and polar dual-axis (Chong and Wong, 2010). Other than dual-axis sun-tracking system, the general formula also can be applied for single-axis tracker; it can be easily obtained by setting secondary angle as constant values. The offset values for each type of sun tracking system are shown in Table 2.1 below.

Table 2.1: Input Offset Parameters for Different Types of Dual-Axis Sun Tracker (Chong and Wong, 2010)

Type of Dual-Axis Sun-Tracking System	Offset parameter (ϕ, λ and ξ)
Azimuth-Elevation	$\phi = 0$, $\lambda = 0$, $\xi = 0$
Polar Dual-Axis	$\phi = 180$, $\lambda = 0$, $\xi = \Phi - 90$

Figure 2.9 shows the ideal azimuth-elevation dual-axis sun-tracking system of collector centre frame (OV, OH and OR axes) with earth surface frame (OZ, OE and ON axes). Furthermore, Figure 2.10 illustrates the process of transformation with respect to three orientation angles.

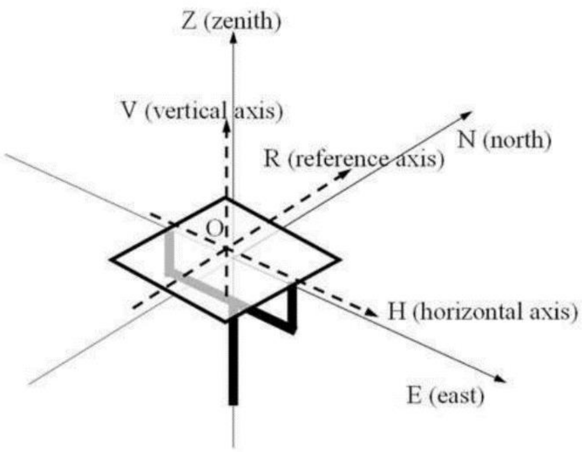

Figure 2.9: Ideal azimuth-elevation dual-axis sun-tracking system with the combination of collector centre frame and earth surface frame (Chong and Wong, 2010)

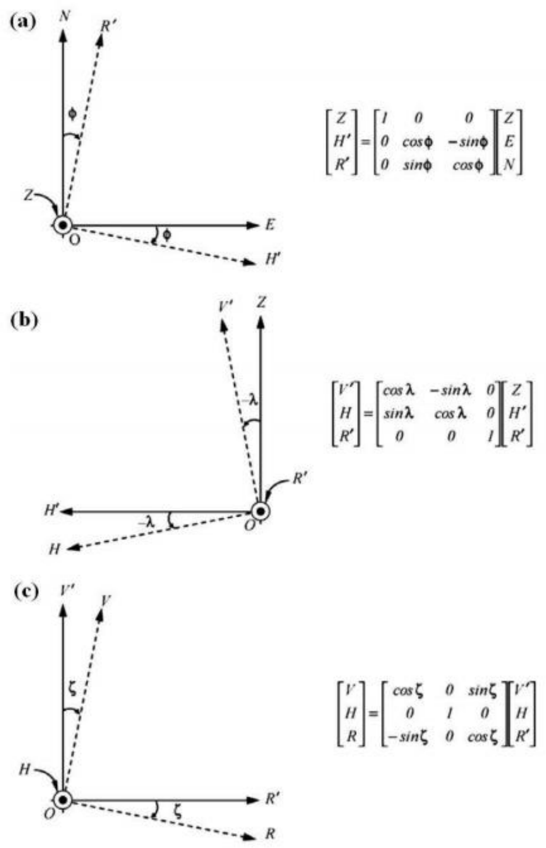

Figure 2.10: The process of coordinate transformation (a) → transformation along the zenith axis (b) transformation along the north axis → (c) transformation along the east axis (Chong and Wong, 2010)

In Figure 2.10 (a), ϕ is the first offset angle to rotate about the zenith axis (OV) of the collector centre coordinate system where it represent the reference orientation of primary axis. For Figure 2.10 (b), λ rotates about the north axis (OR) where Figure 2.10 (c), ξ rotates about the east axis (OH) of the collector centre frame. Figure 2.11 shows the 2D diagram of the combination of collector centre frame axes and earth surface frame axes that eventually contribute to general formula.

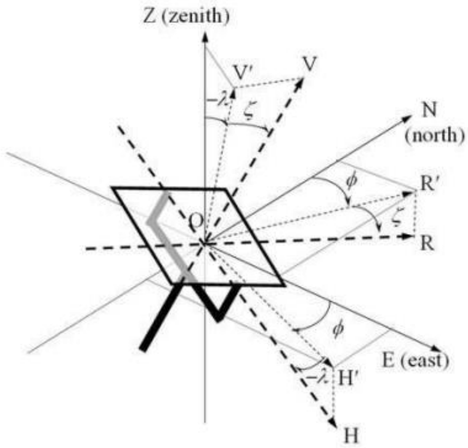

Figure 2.11: The illustration of three rotations in three dimension view interrelated between earth centre frame to the earth surface frame (Chong and Wong, 2010)

The secondary angle of the sun tracking system can be computed by using the equation below:

$$\alpha = arcsin\begin{bmatrix} cos\delta cos\omega(cos\xi cos\lambda cos\Phi - cos\xi sin\lambda sin\phi sin\Phi - sin\xi cos\phi sin\Phi) \\ -cos\delta sin\omega(sin\xi sin\phi - cos\xi sin\lambda cos\phi) \\ +sin\delta(cos\xi cos\lambda sin\Phi + cos\xi sin\lambda sin\phi cos\Phi + sin\xi cos\phi cos\Phi) \end{bmatrix} \quad (2.8)$$

The primary angle can be calculated as follow:

$$cos\beta = \begin{bmatrix} \dfrac{\begin{matrix} cos\delta cos\omega(-sin\xi cos\lambda cos\Phi + sin\xi sin\lambda sin\phi sin\Phi - cos\xi cos\phi sin\Phi) \\ -cos\delta sin\omega(sin\xi sin\lambda cos\phi + cos\xi sin\phi) \\ +sin\delta(-sin\xi cos\lambda sin\Phi - sin\xi sin\lambda sin\phi cos\Phi + cos\xi cos\phi cos\Phi) \end{matrix}}{cos\alpha} \end{bmatrix} \quad (2.9)$$

where

α = secondary angle, °

β = primary angle, °

Due to the fact that the sun position may fall in any four trigonometric quadrants of a particular locations, sine and cosine function must takes into account. The general formula and conditions are as follows.

$$\beta = arcsin\left[\frac{\begin{array}{c}cos\delta cos\omega(sin\lambda cos\Phi + cos\lambda sin\phi sin\Phi)\\ -cos\delta sin\omega cos\lambda cos\phi\\ +sin\delta(sin\lambda sin\Phi - cos\lambda sin\phi cos\Phi)\end{array}}{cos\alpha}\right] \quad (2.10)$$

where $cos\beta \geq 0$

$$\beta = 180 - arcsin\left[\frac{\begin{array}{c}cos\delta cos\omega(sin\lambda cos\Phi + cos\lambda sin\phi sin\Phi)\\ -cos\delta sin\omega cos\lambda cos\phi\\ +sin\delta(sin\lambda sin\Phi - cos\lambda sin\phi cos\Phi)\end{array}}{cos\alpha}\right] \quad (2.11)$$

where $cos\beta < 0$

2.3.2.2 Azimuth-Elevation Dual-Axis Sun-Tracking System

In azimuth-elevation sun-tracking system, the primary axis and secondary axis move freely in any four trigonometric quadrants. The configurations of azimuth-elevation are identify by setting the three orientation angle to $\phi = \xi = \lambda = 0$. Hence, the primary and secondary angles formula can be simplified as follow (Chong and Wong, 2010). Figure 2.12 shows the rotation of primary and secondary axes of azimuth-elevation sun-tracking system.

$$\beta = arcsin\left[-\frac{cos\delta sin\omega}{cos\alpha}\right] \quad (2.12)$$

where $cos\beta \geq 0$

$$\beta = \pi - arcsin\left[-\frac{cos\delta sin\omega}{cos\alpha}\right] \quad (2.13)$$

where $cos\beta < 0$

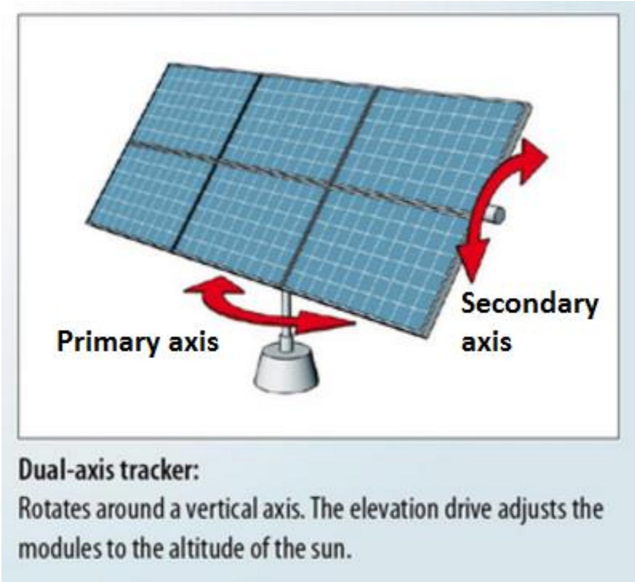

Figure 2.12: Azimuth-elevation Dual-Axis Sun-Tracking System (Nithya, 2015)

2.3.2.3 Polar Dual-Axis Sun-Tracking System

For polar dual-axis tracker, one-axis is automatically tilted to respective latitude angle based on the site location. Polar dual-axis tracker also is known as two-axis equatorial sun-tracking system (Mousazadeh *et al.*, 2009). Figure 2.13 illustrates the primary and secondary axes of the polar dual-axis sun-tracking system. The difference between the polar aligned single-axis and polar (equatorial) dual-axis tracker is that the secondary axis of the polar single-axis is manually predefined before the tracking process start. As for polar (equatorial) dual-axis tracker, the panel automatically tilted to respective latitude angle whenever the tracking system starts operating. The tracker axes configurations obtained by transforming the three orientation angles derived by Chong and Wong, (2010). The three orientation angles for polar dual-axis sun-tracking system transform at $\phi = 180^\circ$, $\lambda = 0^\circ$, $\xi = \Phi - 90^\circ$. After transformation, primary and secondary tracking formula can be simplified and written as follows.

$$\beta = \omega, when - 90^{o} < \omega < 90^{o} \tag{2.14}$$

$$\alpha = \delta \tag{2.15}$$

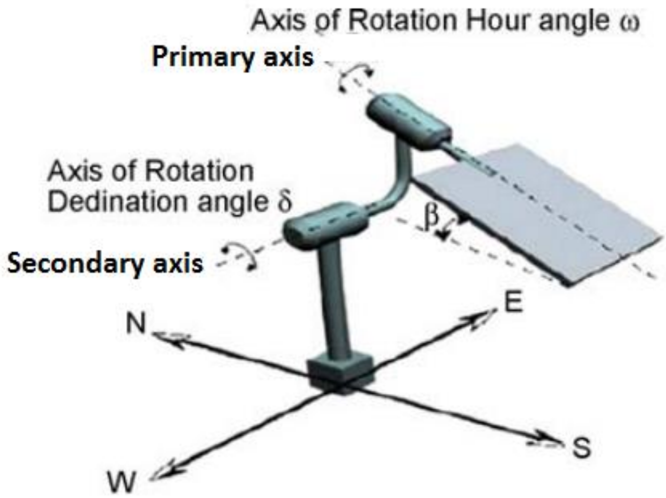

Figure 2.13: Polar Dual-Axis Sun-Tracking System (Mousazadeh *et al.*, 2009)

2.4 Differences between Single-Axis and Dual-Axis Sun-Tracking System

The difference between single-axis and dual-axis sun tracker is that single-axis sun tracker only allows one-axis rotation whereas dual-axis tracker has two axes of rotational angle. The single-axis sun-tracking system has a limitation as it can only track sun movement with one straight path. Unlike single-axis, dual-axis has the ability to track sun position any four trigonometric quadrants (Otieno, 2015). Figure 2.14 below shows the power generation for three type of solar system. It is noticed that dual-axis sun-tracking system has the ability to maximize the energy production as compared to both the fixed tilt and one-axis sun-tracking system.

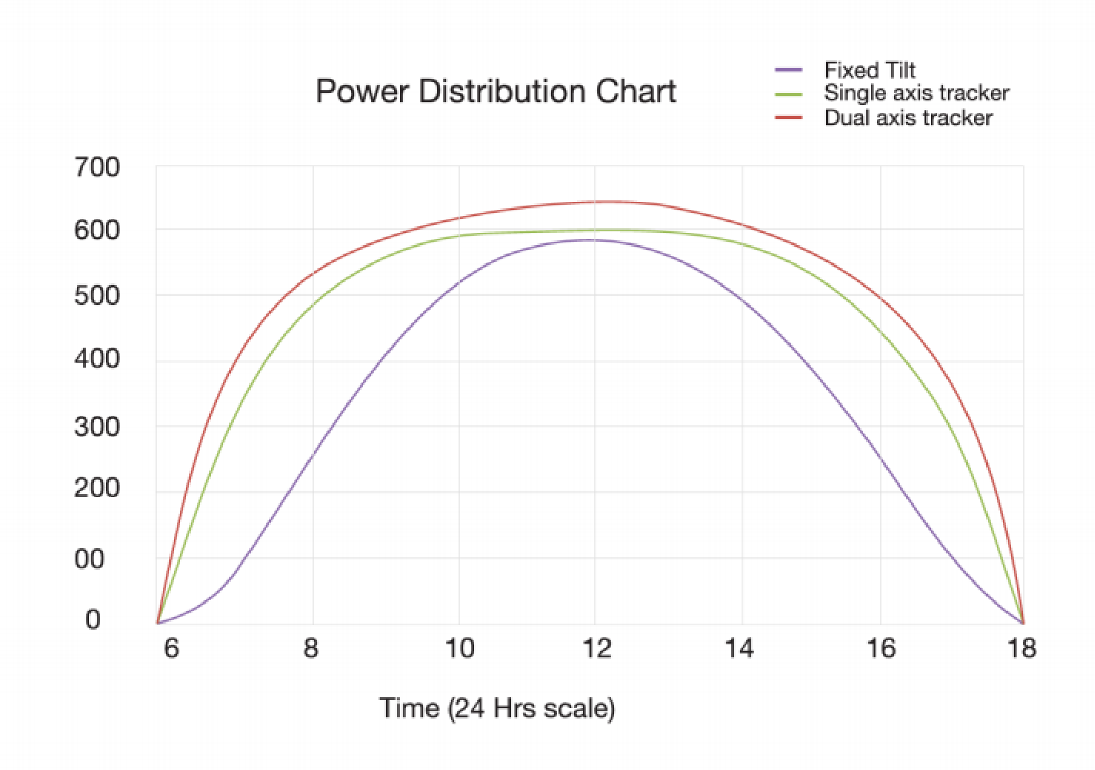

Figure 2.14: Daily Power Generation Comparison between Fixed Mounted, Single-Axis and Dual-Axis Sun-Tracking System (Susten and Road, no date)

2.5 Summary

In short, the dual-axis sun-tracking systems are always the best option in industrial over fixed tilt and single-axis sun-tracking system. As shown in Figure 2.14, the experimental result recorded by (Susten and Road, no date) explained that dual-axis sun-tracking system able to obtain maximum sun irradiance. However, not every location on earth received the same amount of solar irradiation. Thus range of motion must be taken into account. There is a possibility that at certain locations, the motor power consumption is higher than the solar energy being collected. Therefore, the range of motion of each type of dual-axis sun-tracking systems is studied and analysed in the following chapters.

CHAPTER 3

METHODOLOGY AND WORK PLAN

3.1 Introduction

Primary and secondary angles are computed by using the powerful engineering tool, MATLAB. This is to analyse and identify which type of sun-tracking system is the most suitable dual-axis sun-tracking system to be installed at different locations. Other than azimuth-elevation dual-axis sun-tracking system (AE-DAST) and polar dual-axis sun-tracking system (P-DAST), another type of dual-axis sun-tracking system is introduced which is horizontal dual-axis sun-tracking system (H-DAST). The configuration of H-DAST is similar to P-DAST, except for one offset parameter (ξ) it is installed in order to reduce the wind load. Besides that, other than just comparing each type of sun-tracking system, various kind of parameters are introduced and explained in the following sections.

3.2 Types of Dual-Axis Sun-Tracking System

Three types of dual-axis sun-tracking system are considered to compare the accumulated primary and secondary range of motion per annum (AROM). Each tracking system has their own unique characteristic, which is represented by three orientation angles (also known as offset parameters). These three orientation angles defined the type of sun-tracking system being used such as AE-DAST, P-DAST and H-DAST.

Offset parameters for each types of sun-tracking system are as follows:

(i) AE-DAST: ($\phi = 0^\circ$, $\lambda = 0^\circ$, $\xi = 0^\circ$)

(ii) P-DAST ($\phi = 180^\circ$, $\lambda = 0^\circ$, $\xi = \Phi - 90^\circ$)

(iii) H-DAST ($\phi = 180^\circ$, $\lambda = 0^\circ$, $\xi = -90^\circ$)

3.3 Stow Position for Dual-Axis Sun-Tracking System

It is very important to consider stow position for sun-tracking system as the extra range of motion tilted from equatorial plane to first tracking angles will also contribute to the motor power consumption. Two cases of stow position are introduced such as fixed stow and non-fixed stow position in order to compare and justify the suitable type of dual-axis sun-tracking system at different locations.

The primary and secondary fixed stow position are as follows:

(i) AE-DAST: ($\beta = 0^\circ$ & $\alpha = 90^\circ$)

(ii) P-DAST: ($\beta = 0^\circ$ & $\alpha = 2\Phi$)

(iii) H-DAST: ($\beta = 0^\circ$ & $\alpha = 0^\circ$)

The primary and secondary non-fixed stow position are as follows:

(i) AE-DAST: ($\beta = 0^\circ$ & $\alpha = 90^\circ$)

(ii) P-DAST: ($\beta = 0^\circ$ & $\alpha = \Phi$)

(iii) H-DAST: ($\beta = 0^\circ$ & $\alpha = 0^\circ$)

3.3.1 Fixed Stow Position

The above-mentioned stow positions are decided based on the three orientation angles. The three orientation angles for AE-DAST are zero and thus the configuration of the mechanical structure of primary and secondary axes as shown in Figure 2.12 are different as compare to another sun-tracking method. The primary axis is pointing towards OV direction (zenith) where the secondary axis is pointing towards OH (east) direction in the case of collector centre frame without any transformation. Therefore, the parking position of secondary axis is stowed in such a way that the solar panel is parallel to the ground and the angle between the normal of the solar panel and the equatorial horizontal plane is 90°. On the other hand, the configurations of stow position for P-DAST and H-DAST are different from AE-DAST due to non-zero offset values. From the configuration of the polar sun-tracking system, it has different stow position for fixed stow and non-fixed stow positions. For fixed stow position, the secondary angle is set in such a way that panel align parallel with the ground. Therefore the secondary position in the algorithm are set as two times the latitude angle. This means that the panel will be tilted from stow position to designated position and back to initial stow position after complete the tracking process. For fixed stow position, PV tracking system are allowed to return to its fixed position every day. Although more range of motion is required as compare to without stow position, it can reduce the wind load at its maximum. With this advantage, maintenance cost can be reduced and last long.

3.3.2 Non-Fixed Stow Position

Dual-axis sun-tracking PV system non-fixed stow positon is set only for the first day of sun tracking. The panel will only have to tilt from the initial stow position and continue the next day tracking from previous day halted position. Therefore the secondary stow position in the algorithm is set as one latitude angle. This parameter is set in order to reduce the total range of motion which lead to less parasitic loss throughout the year. However this kind of stow position cannot avoid and will continuously experience wind load throughout the year because the position is different every day.

3.4 Starting and Ending Time of the Sun-Tracking Process

The second parameter being introduced to this project is the starting and ending time of the sun tracking process. It is known that the collected sun irradiance is very weak at exactly sunrise or sunset time and thus parasitic loss increased. Therefore it is important to determine the suitable starting and ending time in order to optimize system efficiency. Another algorithm is developed to calculate the angle percentage loss in order to compare and select the suitable starting and ending time for particular latitude. The starting and ending time for the algorithm is set as follows:

(i) LCT_Sunrise + 0 & LCT_Sunset – 0 (Offset = 0 hours)
(ii) LCT_Sunrise + 1 & LCT_Sunset – 1 (Offset = 1 hours)
(iii) LCT_Sunrise + 2 & LCT_Sunset – 2 (Offset = 2 hours)
(iv) LCT_Sunrise + 3 & LCT_Sunset – 3 (Offset = 3 hours)

The starting and ending time condition is set in such a way that the PV system start the sun tracking process delay by one hour and ended earlier by one hour for the case of “LCT_Sunrise + 1 & LCT_Sunset – 1”. The following parameters are repeated by setting 0, 2 and 3 hours whereas 0 hours means maximum range of motion sun-tracking system required from exact sunrise to exact sunset time.

3.5 Net Energy Calculation

Besides study the annual range of motion for various location, energy required by the motors to drive the tracking system were considered in order to calculate the net energy of particular system. Net energy refer to the different between maximum energy able to capture by PV system and energy required to drive the motors. Typical energy generated for selected latitudes were obtained from ASHRAE IWEC2 weather database (*ASHRAE IWEC2 Weather Files*, 2008). In this project, net energy are calculate by consider various parameters from on-axis sun-tracking system such as motor rotational speed (rpm), elevation motor power consumption, gear ratio, azimuth motor power consumption, optical efficiency, electrical conversion efficiency as well as solar concentrator reflective area (Chong and Wong, 2010).

The motor energy consumption of tracking system calculated as follow (Chong and Tan, 2011):

$$\sum E_{motor} = \frac{\sum ROM_{pri}}{\frac{n_{rpm}}{GR} \times 360^{o} \times 60} \times P_{m,p} + \frac{\sum ROM_{sec}}{\frac{n_{rpm}}{GR} \times 360^{o} \times 60} \times P_{m,s} \qquad (3.1)$$

The energy generated from PV system is calculated by using the following formula:

$$\sum E_{gen} = \sum DNI \times A \times \eta_{op} \times \eta_{con} \qquad (3.2)$$

The net energy can be calculated as follow:

$$E_{net} = \sum E_{gen} - \sum E_{motor} \qquad (3.3)$$

where,

DNI = direct normal irradiance, W/m^2

n_{rpm} = 120, rpm

GR = 4400

A = 25, m^2

η_{op} = 85%

η_{op} = 30%

Primary and secondary motor power consumption are assumed based on the specification and energy consumption of prototype, on-axis sun-tracking system (Chong and Wong, 2010). For AE-DAST, secondary axis required more power consumption because the elevation motor required more power to lift up the PV system whereas primary axis require less motor power because it only needs to move around at a fixed point. However, the primary and secondary motor power consumption for P-DAST and H-DAST are assume by interchange primary and secondary motor power consumption. This assumption is made due to more range of motion required by the primary axis in order to elevate the PV system when sun tracking from east to west. Another assumption are made for this project is that the torque required for two motors are the same. The primary and secondary motor power consumption are assume as follows:

(i) AE-DAST ($P_{m,p}$ = 66 W, $P_{m,s}$ = 99 W)

(ii) P-DAST ($P_{m,p}$ = 99 W, $P_{m,s}$ = 66 W)

(iii) H-DAST ($P_{m,p}$ = 99 W, $P_{m,s}$ = 66 W)

3.6 Sun Tracking Algorithm Flowchart

The sun tracking algorithm flowchart illustrates the flows to compute the accumulated primary and secondary angles by considered different parameters throughout the year. In order to calculate the primary and secondary tracking angles, common parameters have to be considered such as latitude angle, longitude angle, daylight saving, time zone meridian and daylight saving. The advantage of using general formula is to study different kinds of sun-tracking systems by changing the offset parameters. After setting the type of sun-tracking system to study, stow position either fixed or non-fixed are selected to study the accumulated range of motion for specific offset time.

The outer for loop of the algorithm is used to determine the accumulated primary and secondary angles from the first day till the last day of the year (N = 1 to 365). Besides that, the inner for loop is used to determine the primary and secondary angles throughout the day with one hour interval. At the end of the simulation, accumulated primary, secondary as well as the total annual accumulated primary and secondary angles are calculated and displayed.

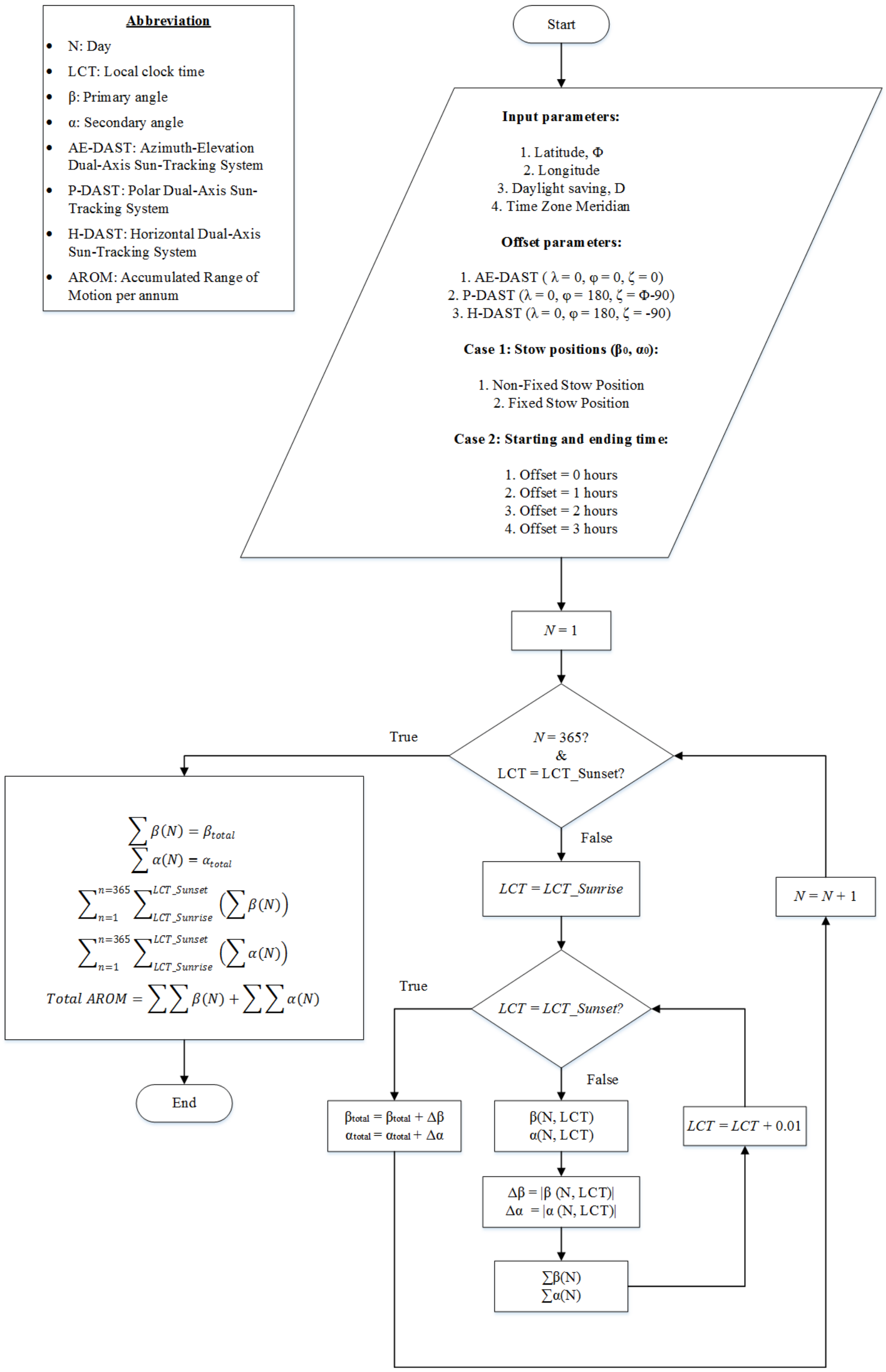

Figure 3.1: Flowchart for Annual Accumulated Range of Motion for each types of Dual-Axis Sun-Tracking System

CHAPTER 4

RESULTS AND DISCUSSIONS

4.1 Daily Accumulated Range of Motion in Malaysia

In this section, daily accumulated primary and secondary range of motion with respect to Malaysia are studied. The trends of each type of dual-axis sun-tracking system for everyday are plotted and analysed with respect to the fixed and non-fixed stow position. For this section, zero offset hours are considered since the trend will be the same for all offset hours except the higher offset hours will have a less daily accumulated range of motion.

4.1.1 Daily Accumulated Range of Motion for Fixed Stow Position

Figure 4.1 below shows the trend of a daily accumulated range of motion for all kinds of dual-axis sun-tracking system with reference fixed stow position in Malaysia. Zero offset hours are considered in this case since the trends for all offset hours are the same, except higher offset hours will have a less daily accumulated range of motion.

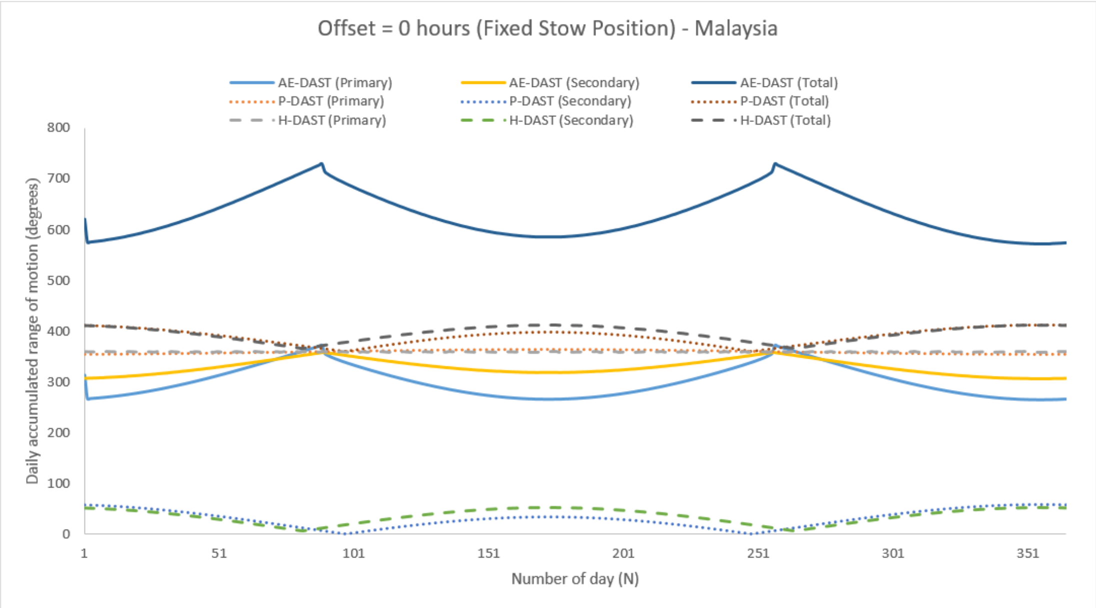

Figure 4.1: Daily Accumulated Range of Motion for each type of Dual-Axis Sun-Tracking System with Fixed Stow Position

It is noticed the range of motion for AE-DAST is the highest among all of the tracking system. The AE-DAST total accumulated range of motion shows that at winter and autumn seasons, the range of motion is less due to shorter sun path or lesser hour of daylight during winter and autumn. At N = 89 (spring) and N = 257 (summer), the range of motion is the highest as compared to other days. This is because of longer sun path across the zenith axis at solar noon. At N = 89, it is the transition of sun path from due south to due north whereas at day N = 257, it is the day where sun path change from the due north direction back to the due south direction.

As comparing P-DAST and H-DAST for stow position, it is noticed that their daily accumulated range of motion throughout the year from N = 1 (1st January) to N = 365 (31st December) is approximately the same. However, H-DAST required slightly more range of motion as compared to P-DAST. This is because of the unique configuration of H-DAST is set in such a way that the PV system is parallel to the ground. Therefore slightly more range of motion is required to direct the PV system towards the sun path throughout the day. As for P-DAST, one of the offset parameters allow the PV system to align with latitude and therefore secondary angle is constant throughout the day. Thus, less motion is required as compared to H-DAST.

Besides that, it is observed that the curve for P-DAST and H-DAST is opposite as compare to AE-DAST. Less range of motion is required for P-DAST and H-DAST at day N = 89 and N = 257 due to the transition from due south direction to de north direction and from due north direction to due south direction respectively as well as stow position. At these day, the PV system does not require much range of motion for primary and secondary axes although it has longer sun path.

The average daily accumulated range of motion for AE-DAST range from 600° to 700° where P-DAST and H-DAST required an average 400° range of motion to maximize the production of solar energy. Therefore it can be deduced that the parasitic losses for P-DAST and H-DAST are less as compared to common used AE-DAST for stow position.

4.1.2 Daily Accumulated Range of Motion for Non-Fixed Stow Position

Figure 4.2 illustrates the daily accumulated range of motion for all kinds of dual-axis sun-tracking systems with reference to the non-fixed stow position. Zero offset hours are considered to study the trend of each sun-tracking system at Malaysia. It is expected that the average daily accumulated range of motion will be lesser as compared to fix stow position.

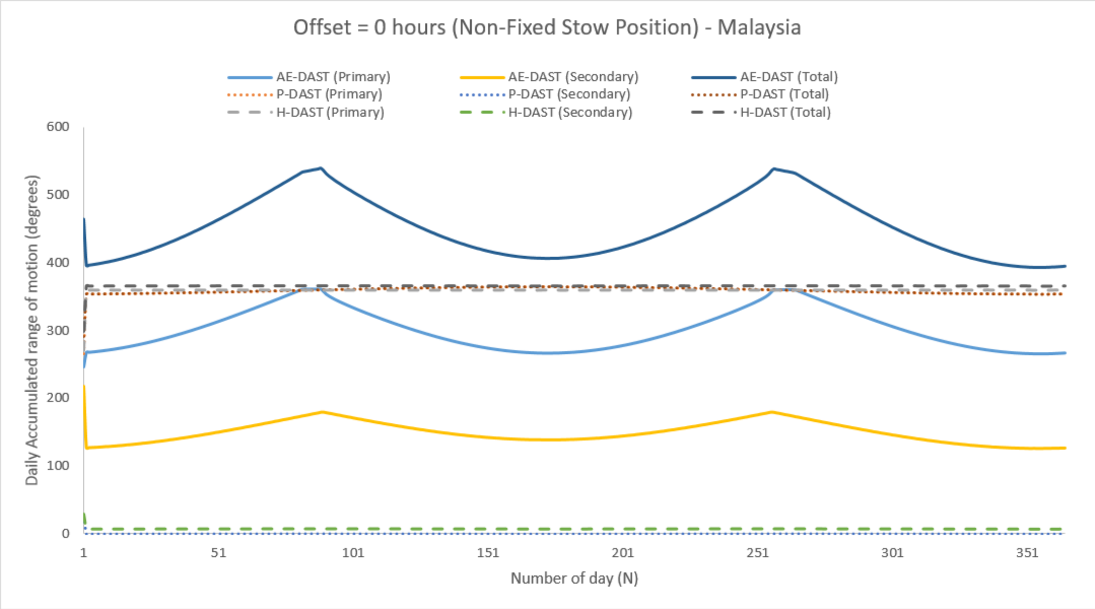

Figure 4.2: Daily Accumulated Range of Motion for each type of Dual-Axis Sun-Tracking System Non-Fixed Stow Position

Figure 4.2 above shows the accumulated range of motion for non-fixed stow position. As expected, AE-DAST required more range of motion as compared to P-DAST and H-DAST in order to harvest maximum solar energy. It is also noticed that the secondary daily accumulated range of motion for P-DAST and H-DAST is almost zero in this case. This is because the PV system only required to tilt about the latitude angle, $\Phi = 3.117^{\circ}$ (Malaysia) from initial stow position and continue the sun-tracking process from previous day halted position. By observing the curve for P-DAST and H-DAST the range of motion throughout the year almost remain unchanged. This is owing to the geographical location of Malaysia in which the sun path limit around the horizon, therefore the PV system does not need to tilt so much for the due south direction and due north direction situations.

4.2 Annual Accumulated Range of Motion for Different Starting and Ending Times

Case 2 is to control the sun-tracking starting and ending times (also known as offset parameter) with respect to various location ranging from 45°N to 45°S. Four curves of the same sun-tracking system are plotted to study the differences between each offset hours in the range of motion.

4.2.1 Annual Accumulated Range of Motion for Fixed Stow Position

Figure 4.3 below shows the trends for different offset hours of all kinds of dual-axis sun-tracking systems with respect to various locations by considering the fixed stow position. With the fixed stow position, it is expected that the annual accumulated range of motion for all kind sun-tracking system required more range of motion as compared to non-fixed stow position due to the additional range of motion required for the PV system to return to its designated stow position.

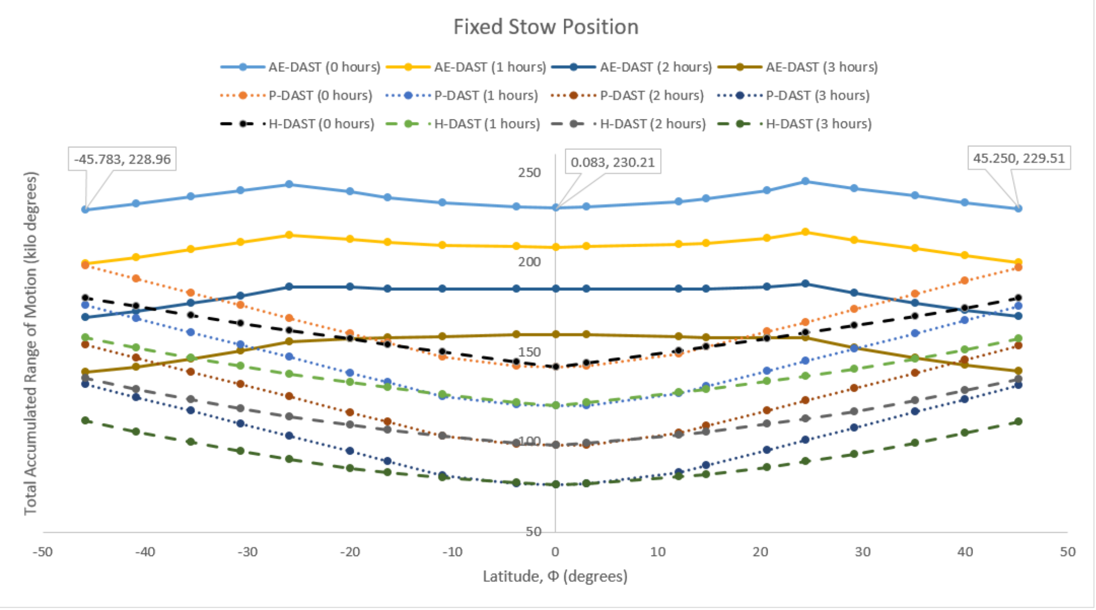

Figure 4.3: Annual Accumulated Range of Motion for each type of Dual-Axis Sun-Tracking System with respect to Various Location (±45◦)

The annual accumulated range of motion for each offset hours with respect to various locations are plotted as shown in Figure 4.3. By observation, it is noticed that the trend for each tracking system ranging for northern and southern hemisphere are symmetrical. It is observed that the annual accumulated range of motion for AE-DAST at 45˚S, 0˚N and 45˚N are around 230000˚, approximately the same but AE-DAST required more range of motion at latitude of 35˚S and 35˚N. The annual accumulated range of motion increase linearly as latitude increased until ±35˚, and decrease steadily from ±35˚ towards ±45˚.

On the other hand, P-DAST and H-DAST experience the same annual accumulated range of motion at latitude, $\Phi = 0^{\circ}$N which is about 140000°. It is observed that, the suitable locations to install P-DAST are the latitudes ranging from 15°S to 15°N due to the lower annual accumulated range of motion as compared to H-DAST. However, latitudes above 15°N and below 15°S are the most suitable places to install H-DAST due to the low annual accumulated range of motion.

For fixed stow position, the annual accumulated range of motion for the P-DAST increases as the latitude is increased from 0°N towards $\pm 45^{\circ}$. The increase in the range of motion is due to the increase of latitude as one of the offset angle ($\xi = \Phi - 90^{\circ}$) required two times latitude angle to return to stow position.

Figure 4.4 demonstrates the percentage difference trend in order to compare the difference in the range of motion of P-DAST and H-DAST with reference to the commonly used AE-DAST.

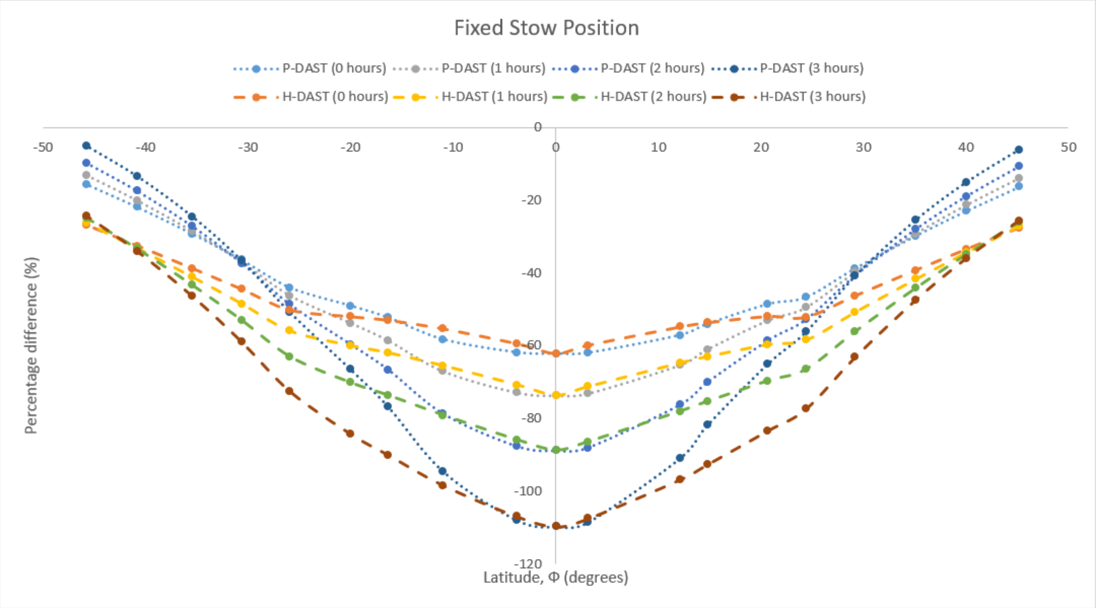

Figure 4.4: Percentage Difference for Various Location with Reference to Azimuth-Elevation Dual-Axis Sun-Tracking System (Fixed Stow Position)

Figure 4.4 compares two tracking system in term of percentage difference with reference to AE-DAST. In term of percentage, it is obvious that AE-DAST required 60% more annual accumulated range of motion to drive the tracking system at latitude, $\Phi = 0^{\circ}$N as compare to P-DAST and H-DAST.

4.2.2 Annual Accumulated Range of Motion for Non-Fixed Stow Position

Figure 4.5 below exhibits the trends for all kinds of dual-axis sun-tracking system for non-fixed stow position with respect to various locations and offset hours.

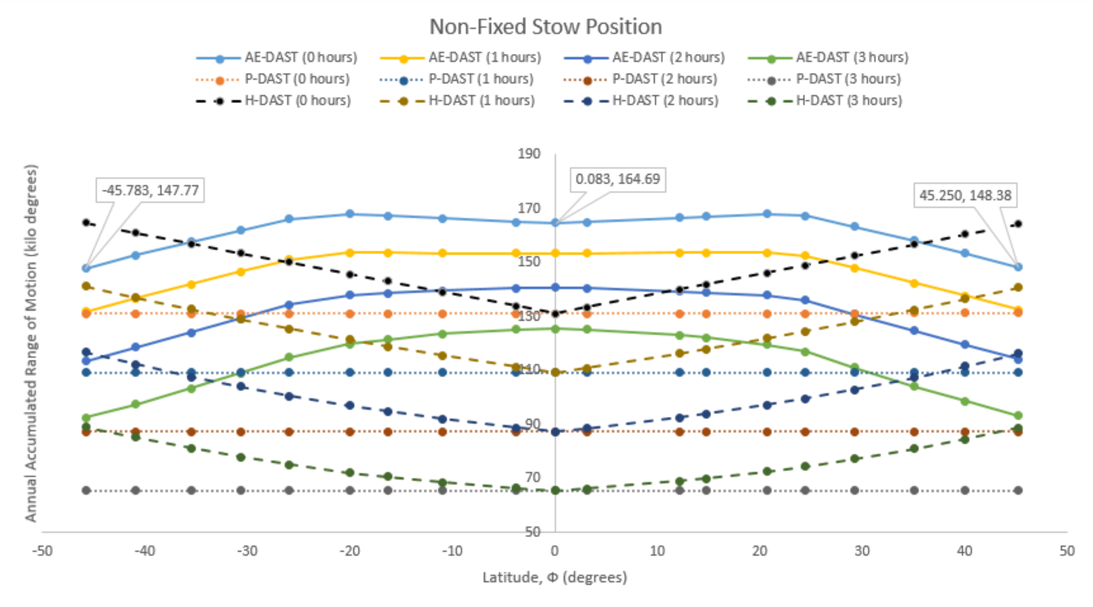

Figure 4.5: Annual Accumulated Range of Motion for each type of Dual-Axis Sun-Tracking System with Respect to Various Locations

For non-fixed stow position, it is observed that the trend for AE-DAST is almost same as the trend plotted for fixed stow position in Figure 4.3. Figure 4.5 shows an annual accumulated range of motion of about 164690˚ much lower as compare to fix stow position (230230˚) in Figure 4.3 for zero offset hours. There is about 28.5% more range of motion required to drive the tracking system if fixed stow parking position is installed at 0.1˚N. In this case, it is noticed that the annual accumulated range of motion at 0.1˚N is larger as compared to 45˚S and 45˚N. As compared to fixed stow position in Figure 4.3, it is because of additional angles required for PV system to return to its designated stow position.

Besides that, P-DAST for non-fixed stow position required the least annual accumulated range of motion throughout the latitude angles from 45˚S to 45˚N for each offset hours. As refer to Figure 4.2, the secondary rotation angles for a daily accumulated range of motion for non-fixed stow position is approximately equal to zero. This means that only accumulated primary angles affect the total accumulated range of motion due to the inherent ability of P-DAST, the offset parameters.

The trend of the annual accumulated range of motion for H-DAST is observed that it increases linearly from the horizon (0°N) towards northern and southern hemisphere. At latitude angle of 35°N and 35°S, it is noticed that there is an overlap between AE-DAST and H-DAST. At latitude above 35°N, AE-DAST has a smaller annual accumulated range of motion as compared to H-DAST. If these two option are considered, the commonly used AE-DAST is a better option. In overall, P-DAST are the best option to consider for non-fixed stow position.

Figure 4.6 demonstrate the difference in range of motion in term of percentage values to identify the suitable sun-tracking system for each location ranging from 45°N to 45°S for non-fixed stow position.

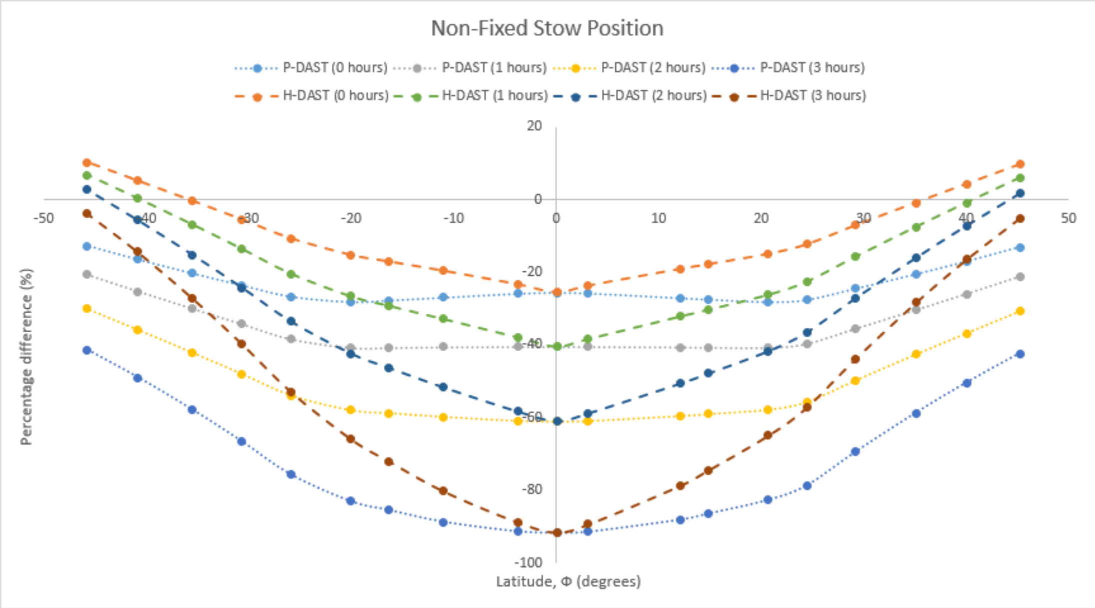

Figure 4.6: Percentage Difference for Various Location with Reference to Azimuth-Elevation Dual-Axis Sun-Tracking System

From the percentage difference curve plotted in Figure 4.6, it is observed that H-DAST required 10% more annual accumulated range of motion for 45°N and 45°S while at 0°N, about 25% less is required for H-DAST as compared to AE-DAST. It is concluded that H-DAST is the best option for latitude angles lower than 35°N and above 35°S. In overall, P-DAST is the best option for all selected latitudes as the percentage difference shows negative values for each offset hours.

4.3 Net Energy and Motor Energy Consumption

Motor energy consumption is essential to consider with respect to the calculated annual accumulated primary and secondary range of motion for various locations. Other than considered the motor energy consumption, energy generated by that particular location has to be considered in other to compute the net energy with respect to offset hours. Net energy is calculated by computing the difference between energy generated and motor energy consumption. It is not suitable to implement the sun-tracking system if that particular location required more motor energy consumption than the generated energy. Table 4.1 below shows the typical amount of direct normal irradiance (DNI) with respect to 19 selected countries around the world.

Table 4.1: Direct Normal Irradiance for Various Location Collected from (*ASHRAE IWEC2 Weather Files*, 2008)

No.	Location	Time Zone	DNI (kWh/m^2)
1	(45.3◦N) ZLIKHA - Kazakhstan	6	1846.42
2	(40.0◦N) SINPO - North Korea	9	1207.47
3	(35.1◦N) BUSAN - South Korea	9	1203.13
4	(29.2◦N) KUWAIT - International Airport	3	1290.79
5	(24.4◦N) ABU DHABI - International Airport	4	1269.30
6	(20.7◦N) AKOLA - Indonesia	5.5	1954.13
7	(14.8◦N) LOPBURI - Thailand	7	1251.01
8	(12.1◦N) NDJAMENA - Africa	1	1898.24
9	(3.1◦N) SUBANG - Malaysia	8	1149.34
10	(0.1◦N) MERU - Kenya	3	1241.16
11	(3.8◦S) FORTALEZA - Brazil	-3	1453.84
12	(11.0◦S) ARACAJU - Brazil	-3	1276.95
13	(16.3◦S) AREQUIPA - Peru	-5	1963.70
14	(20.0◦S) BULAWAYO - Zimbabwe	2	1625.61
15	(25.9◦S) MAVALANE - Mozambique	2	1483.57
16	(30.7◦S) DE-AAR - South Africa	2	2341.94
17	(35.5◦S) MALARGUE - Argentina	-3	1752.54

Table 4.1: (Continued)

18	(40.9◦S) VIEDMA - Argentina	-3	1752.00
19	(45.8◦S) COMODORO-RIVADAVIA - Argentina	-3	1300.29

4.3.1 Net Energy for Fixed Stow Position

Figure 4.7 below illustrates the annual net energy for each dual-axis sun-tracking system with respect to various locations in term of 4 different offset hours. It is noticed that at 30°S which represent De-Arr at South Africa has the highest net energy about 15 MWh as compared to all selected location for all kinds of sun-tracking system.

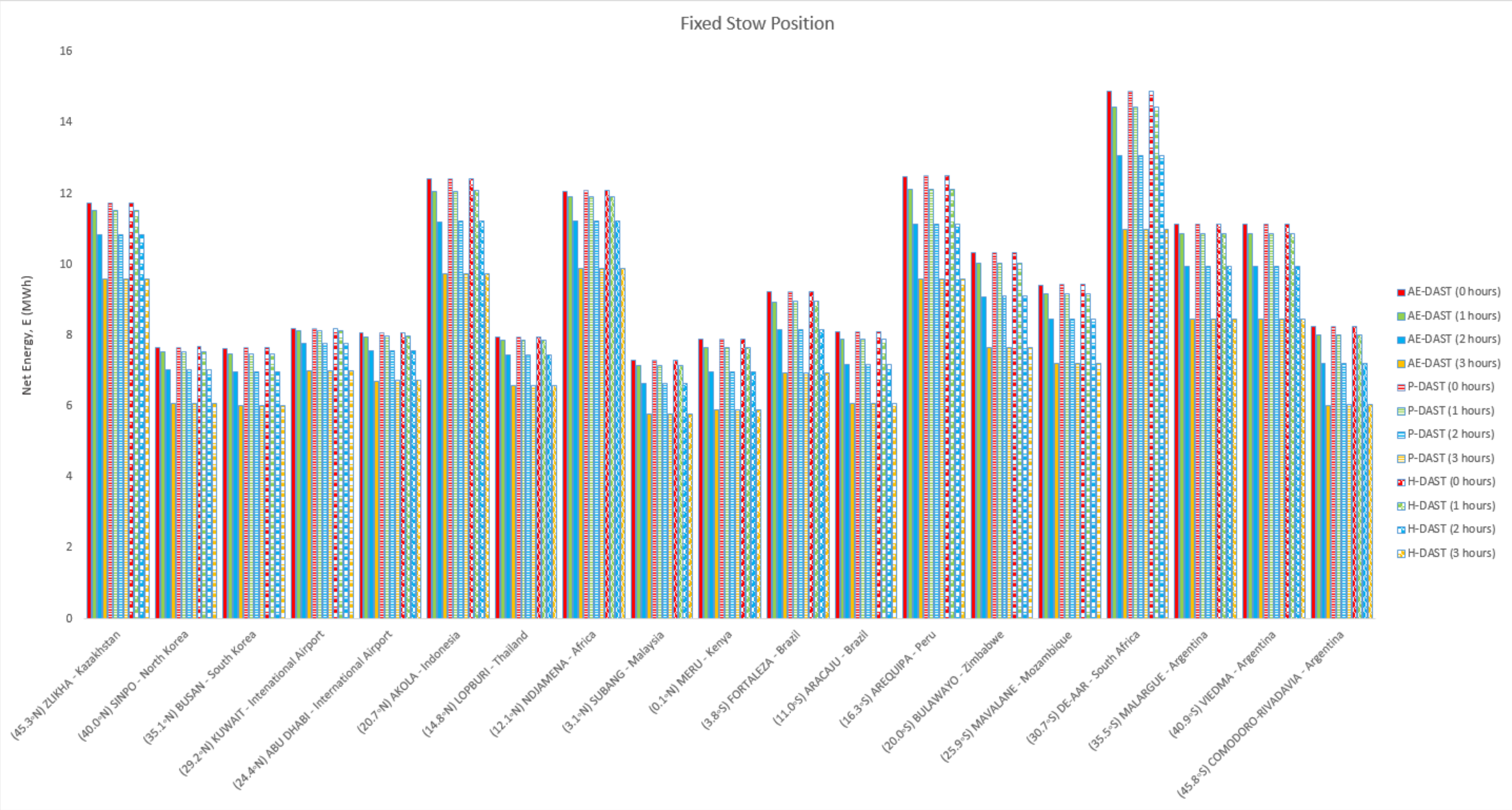

Figure 4.7: Net Energy for each Offset Hours with respect to Various Location

From the bar chart illustrates in Figure 4.7, it is observed that the net energy for all kinds of dual-axis sun-tracking systems for a particular location are the same with respect to different offset hours. Among all the locations, it is noticed that Malaysia has the least net energy (8 MWh) as dual-axis sun-tracking system is installed. With reference to Malaysia case, it is observed that when offset hours increased, the net energy reduced. Offset hours of zero and one shows almost the same net energy while when offset hours increase to two or three, it is noticed that the net energy drop about 1MWh per year. This means that the percentage difference of one offset hours with reference to zero offset hours is less as compare to higher offset hours. This is estimated to be the same for all locations. Therefore, it is deduced that offset hours of three is not suitable to be considered for dual-axis sun-tracking system due to significant losses of energy per year.

By observing the entire bar chart, locations such as Sinpo (40°N) from North Korea, Busan (35°N) from South Korea, Lopburi (14.8°N) from Thailand, Subang (3.1°N) from Malaysia and Aracaju (11°S) from Brazil from Argentina obtained almost the same net energy (about 8 MWh) throughout the year. It is also noticed that location at Kazakhstan, Indonesia, Africa and Peru obtained the most net energy with the least parasitic losses for fixed stow position.

4.3.2 Net Energy for Non-Fixed Stow Position

The bar chart shown in Figure 4.8 illustrates the net energy for a various location with reference to different offset hours. As expected, South Africa with latitude angle, Φ = 30.7°S has the highest net energy as compared to other selected locations with about 15 MWh.

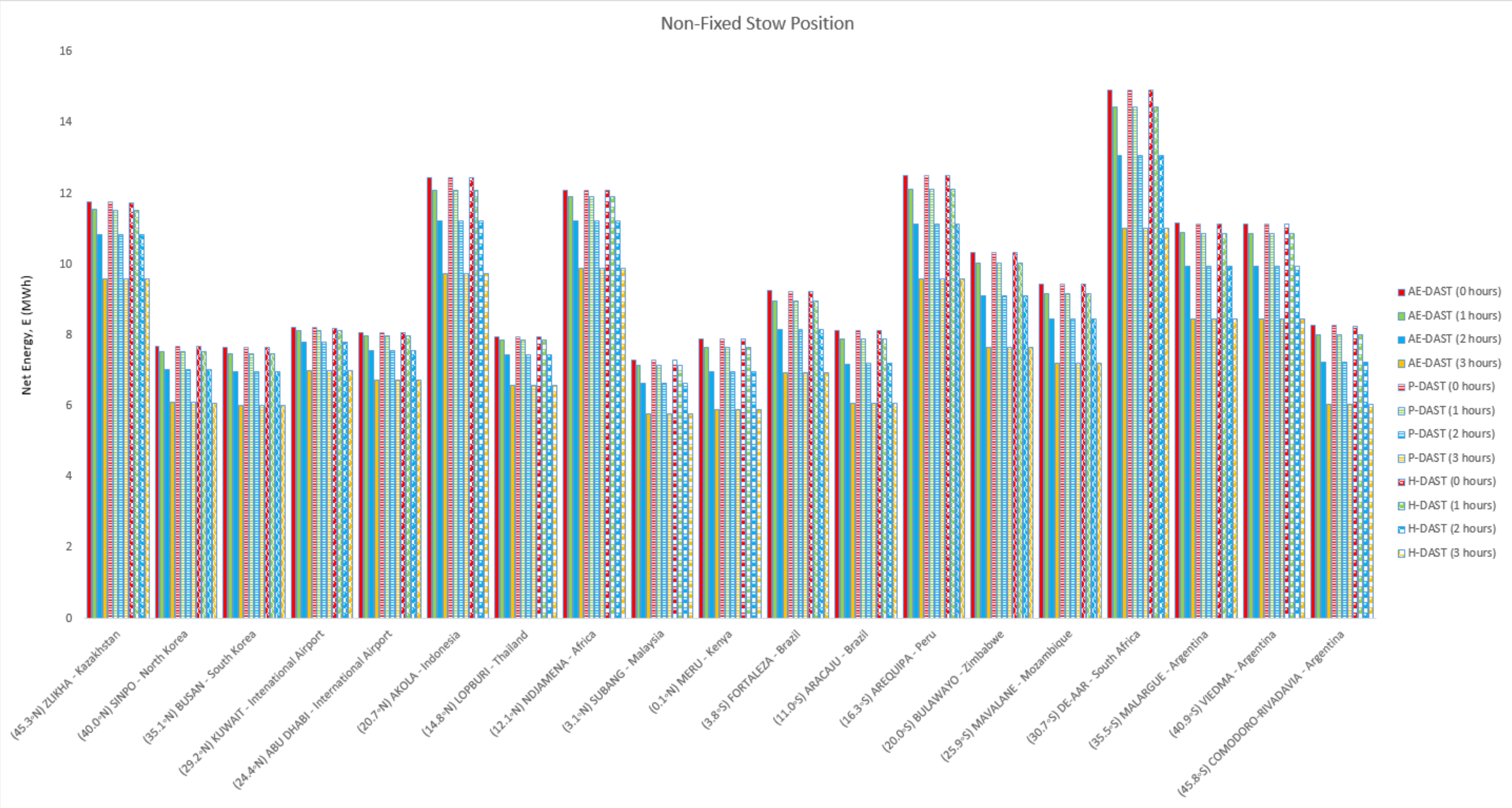

Figure 4.8: Net Energy for each Offset Hours with respect to Various Location

For non-fixed stow position, the trend for the net energy of each dual-axis sun-tracking system with respect to each offset hours are approximately the same as fixed stow-parking position. With reference to the location at De-Arr from South Africa, it is noticed that the net energy difference between two offset hours and three offset hours is about 2 MWh. The net energy difference between offset hours of two and three is about 1 MWh. Although 1MWh of energy loss is significant, two times of net energy losses are more significant for three offset hours. Offset hours of zero or one are the best option to be considered for South Africa.

As comparing latitude angle 35.5°S (Malargue, Argentina) and 40.9°S (Viedma, Argentina), the net energy obtained throughout the year are approximately the same but the energy loss of implementing three hours offset remain unchanged with 2 MWh losses. However, by comparing latitude angle of 30.7°S and 35.5°S, there is only 5° different but the net energy difference is about 5 MWh for each offset hours. This may be due to the geographical difference in the amount of cloud cover that determined the total amount of direct normal irradiance.

In a nutshell, two or three hours offset are not suitable for all selected locations as there will be an energy loss accumulated throughout the year ranging from 1MWh to 5MWh for fixed and non-fixed stow position. Besides that, by comparing fixed and non-fixed stow position, it is noticed that the net energy accumulated throughout the year for each dual-axis sun-tracking system are approximately the same. Therefore fixed stow parking position is the best option to be considered in the design of solar concentrator system because of its ability able to return to designated stow position and thus reduce wind load for the non-tracking period.

4.3.3 Motor Energy Consumption for Fixed and Non-Fixed Stow Position

Figure 4.4 highlight the amount of motor energy consumed by primary and secondary motor for zero offset hours with respect to various location. It is expected that AE-DAST consume more motor power due to the large amount of annual accumulated range of motion required as compared to P-DAST and H-DAST. Only zero offset hours are considered since the pattern will be the same, except the motor energy consumption will decrease as offset hours increase.

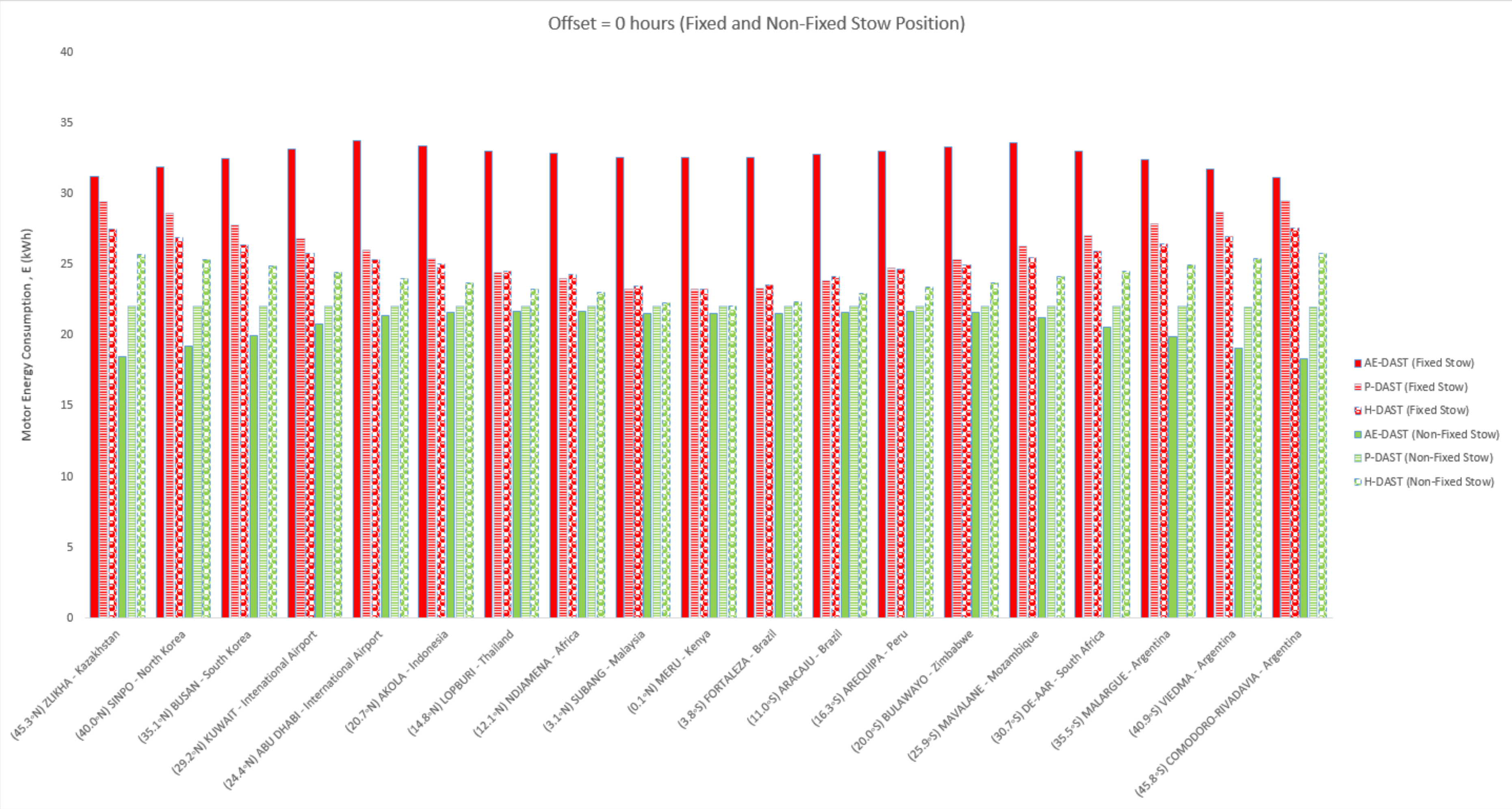

Figure 4.9: Motor Energy Consumption with respect to Various Location

Figure 4.9 shows that AE-DAST required more motor energy consumption as compare to P-DAST and H-DAST. With reference to latitude angle of 24.4°N (Abu Dhabi), AE-DAST required more motor energy as compare to various location. The energies of motors required for fixed and non-fixed stow position are about 33 kWh and 21 kWh respectively. There is about 12 kWh difference of motor energy with the maximum production of solar energy. Therefore it is not viable to implement AE-DAST for his location. By comparing fixed stow position for P-DAST and H-DAST, they required almost the same amount of motor energy to harvest maximum solar energy. Thus, it is concluded that P-DAST and H-DAST with fixed stow position are the best options as compare to AE-DAST at this location. On the other hand, by comparing non-fixed stow position, it is noticed that AE-DAST (21 kWh) required less motor energy as compare to P-DAST (22 kWh) and H-DAST (24 kWh). However, it is noticed that H-DAST required more motor energy consumption for primary and secondary rotational motor.

Besides, the motor energy different at the location at 45°N and 45°S for all kinds of dual-axis sun-tracking system with fixed stow position are small as compare to 24.4°N (Abu Dhabi). This may due to the sun paths are mostly due south or north for 45°N and 45°S respectively. However, the motor energy different for all kinds of tracking systems is large for non-fixed stow position. It is deduced that, H-DAST and AE-DAST for fixed stow position and non-fixed stow position are the better options respectively.

Moreover, for countries located at the horizon (0°) such as Meru fat Kenya (0.1°), there are two best option for fixed stow position which are P-DAST and H-DAST as the motor energy consumption are approximately the same (about 23 kWh) as compare to AE-DAST (about 32 kWh). As for non-fixed stow position, the motor energy consumption for AE-DAST (21 kWh) is relatively less as compared to P-DAST and H-DAST (22 kWh). Therefore AE-DAST is the best option for non-fixed stow position at this location. Since the motor energy consumption for P-DAST and H-DAST for fixed stow position and AE-DAST for non-fixed stow position differ by 2 kWh per year, P-DAST or H-DAST for fixed stow position are recommended as their configuration are able to reduce maximum wind load during the non-tracking period. Therefore less maintenance cost is required although the AE-DAST for non-fixed stow position consume lesser motor energy consumption.

CHAPTER 5

CONCLUSIONS AND RECOMMENDATIONS

5.1 Conclusions

Ultimately, all of the objectives were achieved. Various kinds of dual-axis sun-tracking system are studied by applying the general formula derived by Chong and Wong (2010). Algorithm for azimuth-elevation (AE-DAST), polar (P-DAST) and horizontal (H-DAST) dual-axis sun-tracking system are developed with associated to two cases which are stow position and starting and ending time. Stow position can be further categorised into fixed and non-fixed type. Offset hours (starting and ending time) use to control the tracking starting and ending time are studied based on zero, one, two and three offset hours. Moreover, the performances of all kinds of dual-axis sun-tracking systems are analysed and determine the sun-tracking system with the least parasitic losses to optimize system efficiency.

5.1.1 Fixed Stow Position

In summary, azimuth-elevation dual-axis sun-tracking system (AE-DAST) required an annual accumulated range of motion as large as 60% as compared to polar (P-DAST) and horizontal (H-DAST) dual-axis sun-tracking system.

Besides that, the suitable offset hours for fixed stow position in term of net energy are one offset hours with referenced to zero offset hours because the energy loss is lesser in this case. Offset hours for one, two and three offset hours are within the range of 1% to 3.13%, 5.14% to 12.25% and 17.32% to 26.99% respectively.

Furthermore, suitable types of dual-axis sun-tracking system are determined by analysed the motor energy consumption bar chart shown in Figure 4.9. It is noticed that for latitude ranging from 15°S to 15°N, P-DAST is the best option where H-DAST is the best option to be considered for latitude above 15°N and below 15°S. The most commonly used AE-DAST has relatively large motor energy consumption and therefore it is not one of the option to be implemented.

5.1.2 Non-Fixed Stow Position

In summary, AE-DAST required an annual accumulated range of motion as large as 25% as compare to P-DAST and H-DAST.

Besides that, the suitable offset hours for non-fixed stow position in term of net energy are determined by analysed the net energy bar chart generated as shown in Figure 4.8. With referenced to zero offset hours, one offset hours are the most suitable offset hours to be considered for implementation because the energy loss is lesser. The percentage difference of energy loss is larger for two (5.14% to 12.25%) and three (17.32% to 26.99%) offset hours as compare to one hours offset. The suitable offset hours for non-fixed stow position is the same as fixed stow position.

On the other hand, suitable types of dual-axis sun-tracking system are determined by analysed the motor energy consumption bar chart shown in Figure 4.9. It is noticed that the motor energy consumption for AE-DAST are less as compare to P-DAST and H-DAS for all the selected location especially the difference is clear at the highest latitude of the northern hemisphere and the lowest latitude of the southern hemisphere. The second option of dual-axis sun-tracking system can be considered P-DAST. At the horizon, there are two options can be considered which are P-DAST and H-DAST.

5.2 Recommendations for Future Work

After the comparative study has been done, there are a lot of challenges to be done to verify the simulated result. Other than fixed or non-fixed stow position for all PV system, secondary stow position algorithm can be implemented to study the characteristics of different secondary stow position with respect to various location. Secondary stow position can be set as 30°, 60° and 90°. This condition is set to identify the most suitable secondary stow position to minimize the wind load with respect to various location.

Other than reducing wind load of the sun-tracking system, the experimental result can be obtained by building interchangeable tilt-roll dual-axis sun-tracking system in which the sun-tracking configurations can be easily set by changing the offset parameter. The experimental result can be used to compare with the simulated result.

Furthermore, the experiment can be carried out to identify several assume parameters for P-DAST and H-DAST by implementing a tilt-roll dual-axis sun-tracking system. Values that are assumed in this project are the torque and motor power consumption for the primary and secondary motor.

Other than motor energy consumption, the algorithm to compute the energy consumption of the dual-axis sun-tracking can be further improve by study the mechanical characteristic for all kinds of dual-axis sun-tracking in order to understand the constraint of the system such as parasitic losses.

Lastly, a field layout for more than one dual-axis sun-tracking system can be further study to optimize the system efficiency by minimizing the shadowing effect of the cause by neighbouring PV system. This approach can use to study the optimum area of land use for the various locations.

REFERENCES

Arnab, S., Rachit, V. and Shrikant, B. 2015. Chronological single axis solar tracker. [online] International Journal of Engineering Trends and Technology (IJETT). Available at: http://www.ijettjournal.org/2015/volume-21/number-4/IJETT-V21P236.pdf [Accessed 12 Apr. 2017].

ASHRAE IWEC2 Weather Files (2008). Available at: http://weather.whiteboxtechnologies.com/IWEC2 [Accessed 27 Aug. 2017].

Chong, K. K. and Tan, M. H. (2011) 'Range of motion study for two different sun-tracking methods in the application of heliostat field', Solar Energy, 85(9), pp. 1837–1850. doi: 10.1016/j.solener.2011.04.024 [Accessed 12 Apr. 2017].

Chong, K. and Wong, C. 2010. General formula for on-axis sun-tracking system. solar collectors and panels, theory and applications, [online] 444, pp.274-276. Available at: http://www.intechopen.com/books/solar-collectors-and-panels--theory-andapplications/general-formula-for-on-axis-sun-tracking-system [Accessed 13 Apr. 2017].

Chong, K. and Wong, C. 2010. Open-loop azimuth-elevation sun-tracking system using on-axis general sun-tracking formula for achieving tracking accuracy of below 1 mrad. [online] Kuala Lumpur: Universiti Tunku Abdul Rahman, pp.1-2. Available at: http://ieeexplore.ieee.org.libezp.utar.edu.my/document/5614088/ [Accessed 13 Apr. 2017].

Harb, J. B. O. U. (2012) 'Final year project Acknowledgments', DUAL AXIS SOLAR TRACKER, 53, pp. 5–10. Available at: http://docplayer.net/24995540-Lebanese-university-faculty-of-engineering-ii-final-year-project-telecommunication-engineering-degree-jad-abou-assaly-dual-axis-solar-tracker.html [Accessed 7 Apr. 2017].

IER. 2016. Renewable Energy - IER. [online] Available at: http://instituteforenergyresearch.org/topics/encyclopedia/renewable-energy/ [Accessed 7 Apr. 2017].

Joshua, Z. 2015. Simple Dual Axis Solar Tracker. [online] Instructables.com. Available at: http://www.instructables.com/id/Simple-Dual-Axis-Solar-Tracker/ [Accessed 12 Apr. 2017].

Mousazadeh, H. et al. (2009) 'A review of principle and sun-tracking methods for maximizing solar systems output', Renewable and Sustainable Energy Reviews, 13(8), pp. 1800–1818. doi: 10.1016/j.rser.2009.01.022 [Accessed 7 Apr. 2017].

Narvarte, L. and Lorenzo, E. 2008. Tracking and Ground Cover Ratio. [pdf] Wiley InterScience. Available at: http://www.physics.arizona.edu/~cronin/Solar/References/Shade%20effects/GCR_PIPV2008.pdf [Accessed 12 Apr. 2017].

Nithya (2015) Solar tracker market expected to grow | Evolve India. Available at: http://evolveindia.in/blog/2015/10/24/solar-tracker-market-expected-to-grow/ [Accessed 4 August 2017].

Otieno, O. R. (2015) 'Solar Tracker for Solar Panel,University of Nairobi Faculty', *Solar Tracker for Solar Panel*, 61, pp. 9–11. Available at: http://eie.uonbi.ac.ke/sites/default/files/cae/engineering/eie/SOLAR TRACKER FOR SOLAR PANEL.pdf [Accessed 7 Apr. 2017].

Parmar, N.J., Parmar, A.N. and Gautam, V.S. 2015. Passive solar tracking system. [pdf] International Journal of Emerging Technology and Advanced Engineering. Available at: http://www.ijetae.com/files/Volume5Issue1/IJETAE_0115_21.pdf [Accessed 12 Apr. 2017].

Solar Tracker for Solar Panel, 61, pp. 9–11. Available at: http://eie.uonbi.ac.ke/sites/default/files/cae/engineering/eie/SOLAR TRACKER FOR SOLAR PANEL.pdf [Accessed 8 Apr. 2017].

Susten, M. and Road, M.-M. (no date) 'Solar Photovoltaic (PV) tracking System for Large Scale Solar Power Plants', pp. 1–4. Available at: http://www.mahindrasusten.com/images/pdf/MSAT100.pdf [Accessed 10 Apr. 2017].

Terra Symbiosis. 2000. Exhaustion of fossil fuels. [pdf] Available at: http://www.terra-symbiosis.org/EN_epuisement-fossiles.pdf [Accessed 7 Apr. 2017]

Trieb, F. et al. (2009) 'Global Potential of Concentrating Solar Power', (September), pp. 1–11. Available at: http://www.dlr.de/tt/Portaldata/41/Resources/dokumente/institut/system/publications/Solar_Paces_Paper_Trieb_Final_Colour_corrected.pdf [Accessed 12 Apr. 2017].

Wang, J. and Lu, C. 2013. Design and Implementation of a Sun Tracker with a Dual-Axis Single Motor for an Optical Sensor-Based Photovoltaic System. 1st ed. [ebook] Taiwan, p.3. Available at: http://www.mdpi.com/1424-8220/13/3/3157/pdf [Accessed 12 Apr. 2017].

APPENDICES

APPENDIX A: MATLAB Code

```
%% Dual Axis Sun Tracking System - Azimuth-Elevation Dual Axis Sun
Tracking System
clc
clear

%Input parameters
lat = 3.117;
lon = 101.55;
D = 0;
time_zone_meridian = 120;
LC = (time_zone_meridian-lon)/15;

%Offset parameters
lambda = 0;
phi = 0;
zeta = 0;
park_pri_angle = 0;
park_sec_angle = 90;

%% Fixed Stow Position
N = 1:1:365;
offset = 0;

%Memory preallocation
DA = zeros(length(N),1);
x = zeros(length(N),1);
EOT = zeros(length(N),1);
pri_case_0 = zeros(length(N),1);
sec_case_0 = zeros(length(N),1);
HA_s = zeros(length(N),1);
ts_s = zeros(length(N),1);
HOD = zeros(length(N),1);
LCT_sunrise_actual = zeros(length(N),1);
LCT_sunset_actual = zeros(length(N),1);

pri_now_0 = park_pri_angle;
sec_now_0 = park_sec_angle;

for j = 1:length(N)
   DA(j) = asind(0.39795*cosd(0.98563*(N(j)-173)));
   x(j) = (360*(N(j)-1))/365.242;
   EOT(j) = 0.258*cosd(x(j))-7.461*sind(x(j))-3.648*cosd(2*x(j))-
9.228*sind(2*x(j));
   HA_s(j) = acosd(-tand(DA(j))*tand(lat));
   ts_s(j) = HA_s(j)/15 + 12;
   LCT_sunset_actual(j) = ts_s(j) - (EOT(j)/60) + LC + D;
   HOD(j) = 2*HA_s(j)/15;
   LCT_sunrise_actual(j) = LCT_sunset_actual(j) - HOD(j);

    %Memory preallocation
    %LCT =
floor(LCT_sunrise_actual(j)+1):1:ceil(LCT_sunset_actual(j)-1);
```

```
    LCT =
(LCT_sunrise_actual(j)+0.01)+offset:0.01:(LCT_sunset_actual(j)-
0.01)-offset;
    ts = zeros(length(LCT)+2,1);
    HA = zeros(length(LCT)+2,1);
    sec_0 = zeros(length(LCT)+2,1);
    pri_0 = zeros(length(LCT)+2,1);
    Acc_pri_0 = zeros(length(LCT)+2,1);
    Acc_sec_0 = zeros(length(LCT)+2,1);

    %daily parking position before sunrise
    if N(j) == 1;
        pri_0(1) = 0;
        Acc_pri_0(1) = 0;
    else
        if (DA(j) - lat) < 0    %due south
             pri_0(1) = 180;
             Acc_pri_0(1) = 0;
        else                    %due north
             pri_0(1) = 360;
             Acc_pri_0(1) = 0;
             pri_0(1) = 0;
        end
    end

    sec_0(1) = sec_now_0;

    for i = 2:length(LCT)+1
       ts(i) = LCT(i-1)+(EOT(j)/60) - LC - D;
       HA(i) = 15*(ts(i)-12);

       %To compute secondaty angle (Elevation / altitude)
       A1 = cosd(DA(j))*cosd(HA(i));
       A2 = cosd(zeta)*cosd(lambda)*cosd(lat) -
cosd(zeta)*sind(lambda)*sind(phi)*sind(lat) -
sind(zeta)*cosd(phi)*sind(lat);
       B1 = -cosd(DA(j))*sind(HA(i));
       B2 = sind(zeta)*sind(phi) -
cosd(zeta)*sind(lambda)*cosd(phi);
       C1 = sind(DA(j));
       C2 = cosd(zeta)*cosd(lambda)*sind(lat)+
cosd(zeta)*sind(lambda)*sind(phi)*cosd(lat) +
sind(zeta)*cosd(phi)*cosd(lat);

       sec_0(i) = asind(A1*A2 + B1*B2 + C1*C2);

       %Primary condition equation (Cosine)
       G1 = cosd(DA(j))*cosd(HA(i));
       G2 = -sind(zeta)*cosd(lambda)*cosd(lat) +
sind(zeta)*sind(lambda)*sind(phi)*sind(lat) -
cosd(zeta)*cosd(phi)*sind(lat);
       H1 = -cosd(DA(j))*sind(HA(i));
       H2 = sind(zeta)*sind(lambda)*cosd(phi) +
cosd(zeta)*sind(phi);
       I1 = sind(DA(j));
       I2 = -sind(zeta)*cosd(lambda)*sind(lat) -
sind(zeta)*sind(lambda)*sind(phi)*cosd(lat) +
cosd(zeta)*cosd(phi)*cosd(lat);

       X1 = (G1*G2 + H1*H2 + I1*I2)/cosd(sec_0(i)); %X1 = cos(pri)
```

```
        %Compute primary angle with respective quadrant
        D1 = cosd(DA(j))*cosd(HA(i));
        D2 = sind(lambda)*cosd(lat) +
cosd(lambda)*sind(phi)*sind(lat);
        E1 = -cosd(DA(j))*sind(HA(i))*cosd(lambda)*cosd(phi);
        F1 = sind(DA(j));
        F2 = sind(lambda)*sind(lat) -
cosd(lambda)*sind(phi)*cosd(lat);

        Y1 = (D1*D2 + E1 + F1*F2)/cosd(sec_0(i));     %Y1 = sin(pri)
        Y2 = asind(Y1);                               %Y2 = asind(Y1)

        %Identify the quadrants of sun position
        if X1 < 0
            pri_0(i) = 180-Y2;
        else
            pri_0(i) = Y2;
        end

         %Convert primary angle into positive value
         if pri_0(i) < 0
             pri_0(i) = pri_0(i)+360;
         end

         %Accumulated primary ROM
         if abs(pri_0(i)-pri_0(i-1))>180
            Acc_pri_0(i) = 360-abs(pri_0(i)-pri_0(i-1));
         else
            Acc_pri_0(i) = abs(pri_0(i)-pri_0(i-1));
         end

         Acc_sec_0(i) = abs(sec_0(i) - sec_0(i-1));
    end

         if (DA(j) - lat) < 0     %due south
             pri_0(i+1) = 180;
             Acc_pri_0(i+1) = abs(pri_0(i+1)-pri_0(i));
         else                     %due north
             pri_0(i+1) = 360;
             Acc_pri_0(i+1) =  abs(pri_0(i+1)-pri_0(i));
             pri_0(i+1) = 0;
         end

         sec_0(i+1) = sec_now_0;
         Acc_sec_0(i+1) = abs(sec_0(i+1)-sec_0(i));

    pri_case_0(j) = sum(Acc_pri_0);
    sec_case_0(j) = sum(Acc_sec_0);
end

ROM_pri_0 = sum(pri_case_0);
ROM_sec_0 = sum(sec_case_0);
Total_ROM_0 = ROM_pri_0 + ROM_sec_0;

%% Non-Fixed Stow Position
N = 1:1:365;
offset = 0;

%Memory preallocation
DA = zeros(length(N),1);
x = zeros(length(N),1);
```

```
EOT = zeros(length(N),1);
pri_case_1 = zeros(length(N),1);
sec_case_1 = zeros(length(N),1);
HA_s = zeros(length(N),1);
ts_s = zeros(length(N),1);
HOD = zeros(length(N),1);
LCT_sunrise_actual = zeros(length(N),1);
LCT_sunset_actual = zeros(length(N),1);

pri_now_1 = park_pri_angle;
sec_now_1 = park_sec_angle;

for j = 1:length(N)
   DA(j) = asind(0.39795*cosd(0.98563*(N(j)-173)));
   x(j) = (360*(N(j)-1))/365.242;
   EOT(j) = 0.258*cosd(x(j))-7.461*sind(x(j))-3.648*cosd(2*x(j))-
9.228*sind(2*x(j));
   HA_s(j) = acosd(-tand(DA(j))*tand(lat));
   ts_s(j) = HA_s(j)/15 + 12;
   LCT_sunset_actual(j) = ts_s(j) - (EOT(j)/60) + LC + D;
   HOD(j) = 2*HA_s(j)/15;
   LCT_sunrise_actual(j) = LCT_sunset_actual(j) - HOD(j);

    %Memory preallocation
    %LCT =
floor(LCT_sunrise_actual(j)+1):1:ceil(LCT_sunset_actual(j)-1);
    LCT =
(LCT_sunrise_actual(j)+0.01)+offset:0.01:(LCT_sunset_actual(j)-
0.01)-offset;
    ts = zeros(length(LCT)+2,1);
    HA = zeros(length(LCT)+2,1);
    sec_1 = zeros(length(LCT)+2,1);
    pri_1 = zeros(length(LCT)+2,1);
    Acc_pri_1 = zeros(length(LCT)+2,1);
    Acc_sec_1 = zeros(length(LCT)+2,1);

    %parking position before sunrise
    if N(j) == 1;
        pri_1(1) = pri_now_1;
        sec_1(1) = sec_now_1;
    else
        pri_1(1) = pri_pre_1(end, 1);
        sec_1(1) = sec_pre_1(end, 1);
    end

    for i = 2:length(LCT)+1
       ts(i) = LCT(i-1)+(EOT(j)/60) - LC - D;
       HA(i) = 15*(ts(i)-12);

       %To compute secondaty angle (Elevation / altitude)
       A1 = cosd(DA(j))*cosd(HA(i));
       A2 = cosd(zeta)*cosd(lambda)*cosd(lat) -
cosd(zeta)*sind(lambda)*sind(phi)*sind(lat) -
sind(zeta)*cosd(phi)*sind(lat);
       B1 = -cosd(DA(j))*sind(HA(i));
       B2 = sind(zeta)*sind(phi) -
cosd(zeta)*sind(lambda)*cosd(phi);
       C1 = sind(DA(j));
       C2 = cosd(zeta)*cosd(lambda)*sind(lat)+
cosd(zeta)*sind(lambda)*sind(phi)*cosd(lat) +
sind(zeta)*cosd(phi)*cosd(lat);
```

```
        sec_1(i) = asind(A1*A2 + B1*B2 + C1*C2);

        %Primary condition equation (Cosine)
        G1 = cosd(DA(j))*cosd(HA(i));
        G2 = -sind(zeta)*cosd(lambda)*cosd(lat) +
sind(zeta)*sind(lambda)*sind(phi)*sind(lat) -
cosd(zeta)*cosd(phi)*sind(lat);
        H1 = -cosd(DA(j))*sind(HA(i));
        H2 = sind(zeta)*sind(lambda)*cosd(phi) +
cosd(zeta)*sind(phi);
        I1 = sind(DA(j));
        I2 = -sind(zeta)*cosd(lambda)*sind(lat) -
sind(zeta)*sind(lambda)*sind(phi)*cosd(lat) +
cosd(zeta)*cosd(phi)*cosd(lat);

        X1 = (G1*G2 + H1*H2 + I1*I2)/cosd(sec_1(i)); %X1 = cos(pri)

        %Compute primary angle with respective quadrant
        D1 = cosd(DA(j))*cosd(HA(i));
        D2 = sind(lambda)*cosd(lat) +
cosd(lambda)*sind(phi)*sind(lat);
        E1 = -cosd(DA(j))*sind(HA(i))*cosd(lambda)*cosd(phi);
        F1 = sind(DA(j));
        F2 = sind(lambda)*sind(lat) -
cosd(lambda)*sind(phi)*cosd(lat);

        Y1 = (D1*D2 + E1 + F1*F2)/cosd(sec_1(i));    %Y1 = sin(pri)
        Y2 = asind(Y1);                              %Y2 = asind(Y1)

        %Identify the quadrants of sun position
        if X1 < 0
            pri_1(i) = 180-Y2;
        else
            pri_1(i) = Y2;
        end

         %Convert primary angle into positive value
         if pri_1(i) < 0
             pri_1(i) = pri_1(i)+360;
         end

         %Accumulated primary ROM
         if abs(pri_1(i)-pri_1(i-1))>180
            Acc_pri_1(i) = 360-abs(pri_1(i)-pri_1(i-1));
         else
            Acc_pri_1(i) = abs(pri_1(i)-pri_1(i-1));
         end

         Acc_sec_1(i) = abs(sec_1(i) - sec_1(i-1));
    end

    pri_1(i+1) = abs(pri_1(i+1)-pri_1(i));
    sec_1(i+1) = abs(sec_1(i+1)-sec_1(i));

    sec_pre_1 = sec_1(end,1);
    pri_pre_1 = pri_1(end,1);

    pri_case_1(j) = sum(Acc_pri_1);
    sec_case_1(j) = sum(Acc_sec_1);
end
```

```
ROM_pri_1 = sum(pri_case_1);
ROM_sec_1 = sum(sec_case_1);
Total_ROM_1 = ROM_pri_1 + ROM_sec_1;

%% Dual Axis Sun Tracking System - Polar and Horizontal Dual-Axis
sun-Tracking System
clc
clear

%Input parameters
lat = 3.117;
lon = 101.55;
D = 0;
time_zone_meridian = 120;
LC = (time_zone_meridian-lon)/15;

%Offset parameters
%Polar Dual Axis Sun Tracking System
lambda = 0;
phi = 180;
zeta = lat-90;
park_pri_angle = 0;
park_sec_angle = 0+2*lat;

%Horizontal Dual Axis Sun Tracking System
% lambda = 0;
% phi = 180;
% zeta = -90;
% park_pri_angle = 0;
% park_sec_angle = 0;

%% Fixed Stow Position
N = 1:1:365;
offset = 0;

%Memory preallocation
DA = zeros(length(N),1);
x = zeros(length(N),1);
EOT = zeros(length(N),1);
pri_case_0 = zeros(length(N),1);
sec_case_0 = zeros(length(N),1);
HA_s = zeros(length(N),1);
ts_s = zeros(length(N),1);
HOD = zeros(length(N),1);
LCT_sunrise_actual = zeros(length(N),1);
LCT_sunset_actual = zeros(length(N),1);

pri_now_0 = park_pri_angle;
sec_now_0 = park_sec_angle;

for j = 1:length(N)
   DA(j) = asind(0.39795*cosd(0.98563*(N(j)-173)));
   x(j) = (360*(N(j)-1))/365.242;
   EOT(j) = 0.258*cosd(x(j))-7.461*sind(x(j))-3.648*cosd(2*x(j))-
9.228*sind(2*x(j));
   HA_s(j) = acosd(-tand(DA(j))*tand(lat));
   ts_s(j) = HA_s(j)/15 + 12;
   LCT_sunset_actual(j) = ts_s(j) - (EOT(j)/60) + LC + D;
   HOD(j) = 2*HA_s(j)/15;
   LCT_sunrise_actual(j) = LCT_sunset_actual(j) - HOD(j);
```

```
    %Memory preallocation
    %LCT =
floor(LCT_sunrise_actual(j)+1):1:ceil(LCT_sunset_actual(j)-1);
    LCT =
(LCT_sunrise_actual(j)+0.01)+offset:0.01:(LCT_sunset_actual(j)-
0.01)-offset;
    ts = zeros(length(LCT)+2,1);
    HA = zeros(length(LCT)+2,1);
    sec_0 = zeros(length(LCT)+2,1);
    pri_0 = zeros(length(LCT)+2,1);
    Acc_pri_0 = zeros(length(LCT)+2,1);
    Acc_sec_0 = zeros(length(LCT)+2,1);

    %daily parking position before sunrise
    pri_0(1) = pri_now_0;
    sec_0(1) = sec_now_0;

    for i = 2:length(LCT)+1
       ts(i) = LCT(i-1)+(EOT(j)/60) - LC - D;
       HA(i) = 15*(ts(i)-12);

       %To compute secondaty angle (Elevation / altitude)
       A1 = cosd(DA(j))*cosd(HA(i));
       A2 = cosd(zeta)*cosd(lambda)*cosd(lat) -
cosd(zeta)*sind(lambda)*sind(phi)*sind(lat) -
sind(zeta)*cosd(phi)*sind(lat);
       B1 = -cosd(DA(j))*sind(HA(i));
       B2 = sind(zeta)*sind(phi) -
cosd(zeta)*sind(lambda)*cosd(phi);
       C1 = sind(DA(j));
       C2 = cosd(zeta)*cosd(lambda)*sind(lat)+
cosd(zeta)*sind(lambda)*sind(phi)*cosd(lat) +
sind(zeta)*cosd(phi)*cosd(lat);

       sec_0(i) = asind(A1*A2 + B1*B2 + C1*C2);

       %Primary condition equation (Cosine)
       G1 = cosd(DA(j))*cosd(HA(i));
       G2 = -sind(zeta)*cosd(lambda)*cosd(lat) +
sind(zeta)*sind(lambda)*sind(phi)*sind(lat) -
cosd(zeta)*cosd(phi)*sind(lat);
       H1 = -cosd(DA(j))*sind(HA(i));
       H2 = sind(zeta)*sind(lambda)*cosd(phi) +
cosd(zeta)*sind(phi);
       I1 = sind(DA(j));
       I2 = -sind(zeta)*cosd(lambda)*sind(lat) -
sind(zeta)*sind(lambda)*sind(phi)*cosd(lat) +
cosd(zeta)*cosd(phi)*cosd(lat);

       X1 = (G1*G2 + H1*H2 + I1*I2)/cosd(sec_0(i)); %X1 = cos(pri)

       %Compute primary angle with respective quadrant
       D1 = cosd(DA(j))*cosd(HA(i));
       D2 = sind(lambda)*cosd(lat) +
cosd(lambda)*sind(phi)*sind(lat);
       E1 = -cosd(DA(j))*sind(HA(i))*cosd(lambda)*cosd(phi);
       F1 = sind(DA(j));
       F2 = sind(lambda)*sind(lat) -
cosd(lambda)*sind(phi)*cosd(lat);
```

```
        Y1 = (D1*D2 + E1 + F1*F2)/cosd(sec_0(i));       %Y1 = sin(pri)
        Y2 = asind(Y1);                                 %Y2 = asind(Y1)

        %Identify the quadrants of sun position
        if X1 < 0
            pri_0(i) = 180-Y2;
        else
            pri_0(i) = Y2;
        end

         %Convert primary angle into positive value
         if HA(i) < 0
             if pri_0(i)>90
                 pri_0(i) = pri_0(i)-360;
             end
         else
              if  pri_0(i)<-90
                  pri_0(i) =  pri_0(i)+360;
             end
         end

         %Accumulated primary ROM
         if abs(pri_0(i)-pri_0(i-1))>180
            Acc_pri_0(i) = 360-abs(pri_0(i)-pri_0(i-1));
         else
            Acc_pri_0(i) = abs(pri_0(i)-pri_0(i-1));
         end

         Acc_sec_0(i) = abs(sec_0(i) - sec_0(i-1));

    end

         pri_0(i+1) = pri_now_0;
         Acc_pri_0(i+1) =  abs(pri_0(i+1)-pri_0(i));
         sec_0(i+1) = sec_now_0;
         Acc_sec_0(i+1) = abs(sec_0(i+1)-sec_0(i));

    pri_case_0(j) = sum(Acc_pri_0);
    sec_case_0(j) = sum(Acc_sec_0);
end

ROM_pri_0 = sum(pri_case_0);
ROM_sec_0 = sum(sec_case_0);
Total_ROM_0 = ROM_pri_0 + ROM_sec_0;

%% "Non-Fixed Stow Position
N = 1:1:365;
offset = 0;

%Memory preallocation
DA = zeros(length(N),1);
x = zeros(length(N),1);
EOT = zeros(length(N),1);
pri_case_1 = zeros(length(N),1);
sec_case_1 = zeros(length(N),1);
HA_s = zeros(length(N),1);
ts_s = zeros(length(N),1);
HOD = zeros(length(N),1);
LCT_sunrise_actual = zeros(length(N),1);
LCT_sunset_actual = zeros(length(N),1);
```

```
pri_now_1 = park_pri_angle;
sec_now_1 = park_sec_angle;

for j = 1:length(N)
   DA(j) = asind(0.39795*cosd(0.98563*(N(j)-173)));
   x(j) = (360*(N(j)-1))/365.242;
   EOT(j) = 0.258*cosd(x(j))-7.461*sind(x(j))-3.648*cosd(2*x(j))-
9.228*sind(2*x(j));
   HA_s(j) = acosd(-tand(DA(j))*tand(lat));
   ts_s(j) = HA_s(j)/15 + 12;
   LCT_sunset_actual(j) = ts_s(j) - (EOT(j)/60) + LC + D;
   HOD(j) = 2*HA_s(j)/15;
   LCT_sunrise_actual(j) = LCT_sunset_actual(j) - HOD(j);

    %Memory preallocation
    %LCT =
floor(LCT_sunrise_actual(j)+1):1:ceil(LCT_sunset_actual(j)-1);
    LCT =
(LCT_sunrise_actual(j)+0.01)+offset:0.01:(LCT_sunset_actual(j)-
0.01)-offset;
    ts = zeros(length(LCT)+2,1);
    HA = zeros(length(LCT)+2,1);
    sec_1 = zeros(length(LCT)+2,1);
    pri_1 = zeros(length(LCT)+2,1);
    Acc_pri_1 = zeros(length(LCT)+2,1);
    Acc_sec_1 = zeros(length(LCT)+2,1);

    %parking position before sunrise
    if N(j) == 1;
        pri_1(1) = pri_now_1;
        sec_1(1) = sec_now_1;
    else
        pri_1(1) = pri_pre_1(end, 1);
        sec_1(1) = sec_pre_1(end, 1);
    end

    for i = 2:length(LCT)+1
       ts(i) = LCT(i-1)+(EOT(j)/60) - LC - D;
       HA(i) = 15*(ts(i)-12);

       %To compute secondaty angle (Elevation / altitude)
       A1 = cosd(DA(j))*cosd(HA(i));
       A2 = cosd(zeta)*cosd(lambda)*cosd(lat) -
cosd(zeta)*sind(lambda)*sind(phi)*sind(lat) -
sind(zeta)*cosd(phi)*sind(lat);
       B1 = -cosd(DA(j))*sind(HA(i));
       B2 = sind(zeta)*sind(phi) -
cosd(zeta)*sind(lambda)*cosd(phi);
       C1 = sind(DA(j));
       C2 = cosd(zeta)*cosd(lambda)*sind(lat)+
cosd(zeta)*sind(lambda)*sind(phi)*cosd(lat) +
sind(zeta)*cosd(phi)*cosd(lat);

       sec_1(i) = asind(A1*A2 + B1*B2 + C1*C2);

       %Primary condition equation (Cosine)
       G1 = cosd(DA(j))*cosd(HA(i));
       G2 = -sind(zeta)*cosd(lambda)*cosd(lat) +
sind(zeta)*sind(lambda)*sind(phi)*sind(lat) -
cosd(zeta)*cosd(phi)*sind(lat);
       H1 = -cosd(DA(j))*sind(HA(i));
```

```
        H2 = sind(zeta)*sind(lambda)*cosd(phi) +
cosd(zeta)*sind(phi);
        I1 = sind(DA(j));
        I2 = -sind(zeta)*cosd(lambda)*sind(lat) -
sind(zeta)*sind(lambda)*sind(phi)*cosd(lat) +
cosd(zeta)*cosd(phi)*cosd(lat);

        X1 = (G1*G2 + H1*H2 + I1*I2)/cosd(sec_1(i)); %X1 = cos(pri)

        %Compute primary angle with respective quadrant
        D1 = cosd(DA(j))*cosd(HA(i));
        D2 = sind(lambda)*cosd(lat) +
cosd(lambda)*sind(phi)*sind(lat);
        E1 = -cosd(DA(j))*sind(HA(i))*cosd(lambda)*cosd(phi);
        F1 = sind(DA(j));
        F2 = sind(lambda)*sind(lat) -
cosd(lambda)*sind(phi)*cosd(lat);

        Y1 = (D1*D2 + E1 + F1*F2)/cosd(sec_1(i));    %Y1 = sin(pri)
        Y2 = asind(Y1);                              %Y2 = asind(Y1)

        %Identify the quadrants of sun position
        if X1 < 0
            pri_1(i) = 180-Y2;
        else
            pri_1(i) = Y2;
        end

        %Convert primary angle into positive value
         if HA(i) < 0
             if pri_1(i)>90
                 pri_1(i) = pri_1(i)-360;
             end
         else
              if  pri_1(i)<-90
                  pri_1(i) =  pri_1(i)+360;
             end
         end

         %Accumulated primary ROM
         if abs(pri_1(i)-pri_1(i-1))>180
            Acc_pri_1(i) = 360-abs(pri_1(i)-pri_1(i-1));
         else
            Acc_pri_1(i) = abs(pri_1(i)-pri_1(i-1));
         end

         Acc_sec_1(i) = abs(sec_1(i) - sec_1(i-1));
    end

    Acc_pri_1(i+1) =  abs(pri_1(i+1)-pri_1(i));
    Acc_sec_1(i+1) = abs(sec_1(i+1)-sec_1(i));

    pri_1(i+1) = pri_1(i);
    sec_1(i+1) = sec_1(i);

    sec_pre_1 = sec_1(end,1);
    pri_pre_1 = pri_1(end,1);

    pri_case_1(j) = sumabs(diff(pri_1));
    sec_case_1(j) = sumabs(diff(sec_1));
end
```

```
ROM_pri_1 = sum(pri_case_1);
ROM_sec_1 = sum(sec_case_1);
Total_ROM_1 = ROM_pri_1 + ROM_sec_1;
```